LBNL-39592

Ernest Orlando Lawrence Berkeley National Laboratory

Flow Channeling in Heterogeneous Fractured Rocks

Chin-Fu Tsang and Ivars Neretnieks

Earth Sciences Division

October 1997

Accepted for publication in *Reviews of Geophysics*

REFERENCE COPY
Does Not
Circulate
Bldg. 50 Library - Ref.
Lawrence Berkeley National Laboratory
Copy 1
LBNL-39592

DISCLAIMER

This document was prepared as an account of work sponsored by the United States Government. While this document is believed to contain correct information, neither the United States Government nor any agency thereof, nor the Regents of the University of California, nor any of their employees, makes any warranty, express or implied, or assumes any legal responsibility for the accuracy, completeness, or usefulness of any information, apparatus, product, or process disclosed, or represents that its use would not infringe privately owned rights. Reference herein to any specific commercial product, process, or service by its trade name, trademark, manufacturer, or otherwise, does not necessarily constitute or imply its endorsement, recommendation, or favoring by the United States Government or any agency thereof, or the Regents of the University of California. The views and opinions of authors expressed herein do not necessarily state or reflect those of the United States Government or any agency thereof or the Regents of the University of California.

Accepted for publication in
Reviews of Geophysics
December 1997

LBNL-39592

Flow Channeling in Heterogeneous Fractured Rocks

Chin-Fu Tsang[1] and Ivars Neretnieks[2]

[1]Earth Sciences Division
Ernest Orlando Lawrence Berkeley National Laboratory
University of California
Berkeley, California 94720

[2]Department of Chemical Engineering
Royal Institute of Technology
10044 Stockholm, Sweden

October 1997

The paper is prepared with the joint support of the Nuclear Power and Fuel Development Corporation (PNC), Japan, and the Office of Energy Research, Office of Basic Energy Sciences, Engineering and Geosciences Division, of the U.S. Department of Energy under Contract No. DE-AC03-76SF00098.

Flow Channeling in Heterogeneous Fractured Rocks

Chin-Fu Tsang[1] and Ivars Neretnieks[2]

[1]Earth Sciences Division
Ernest Orlando Lawrence Berkeley National Laboratory
University of California
Berkeley, California 94720

[2]Department of Chemical Engineering
Royal Institute of Technology
10044 Stockholm, Sweden

October 1997

Abstract

Experimental observations and theoretical studies over the last ten years or so have demonstrated that flow channeling or preferred flow paths is a common phenomenon in fractured rocks. The reason it has come to the forefront of scientific investigation is the recent interest in predicting solute transport in geological media, as part of safety assessment of geologic isolation of nuclear or toxic wastes. Solute transport is much more sensitive to medium heterogeneity than temperature or pressure. In this paper, experimental observations of tracer transport over distances ranging from centimeters to hundreds of meters are reviewed, and theoretical efforts to explain or model these observations are summarized. Processes that may explain some of the experimental observations without the use of flow channeling models are discussed. Finally, the paper concludes with a discussion of the implications of flow channeling on the practical problems related to contaminant transport in geologic systems.

Introduction

The study of fluid flow and solute transport in heterogeneous fractured rocks has been of much interest in recent years (see, for example, Bear et al., 1993; National Research Council, 1996). Its importance lies in the need to predict these processes in geological formations, which may be used for the disposal of nuclear or toxic wastes (National Research Council, 1984; Kobus et al., 1996; Nuclear Energy Agency, 1996; Witherspoon, 1996).

Flow and transport in geological formations are often calculated assuming that geological formations are homogeneous. Based on this, various theories and equations have been developed, including the well-known advective dispersive equation and its solutions (see e.g., Javandel et al., 1984). However, it is recognized that rock contains fractures both as major faults and as smaller and shorter fractures that significantly influence flow and transport. This has motivated Long et al. (1982), Andersson and Dverstorp (1987), Dverstorp and Andersson (1989), Endo et al. (1984), Dershowitz and Schrauf (1987), and others to develop fracture network models. In these models, it is typically assumed that the rock matrix is impermeable except for a fracture network composed of cracks with a uniform aperture. Recent work, both theoretical and experimental, has shown that these models are not adequate to describe the characteristics of flow and transport in many real systems, and much work has since been done to take into account the heterogeneous characteristics of the apertures within each fracture in the network and of the distribution of hydraulic properties of the rock matrix.

In considering the temperature distribution in geological systems such as in the study of geothermal heat flow and in geothermal reservoir analysis, heterogeneity is not very important, because heat conduction will smooth out the property variations. If one is interested in the pressure distribution in a geological formation such as in the analysis of well test data and in the evaluation of aquifer or reservoir capacities, one finds that

the result is sensitive to major features such as large fracture zones or formation stratification, but is not sensitive to smaller heterogeneities. However, in solving problems of solute transport in a geological formation, the results are usually much more sensitive to both small and large scale heterogeneity.

By flow channeling, we refer to the phenomenon that liquid flow through a geologic system with its heterogeneous structure is focused in a rock fracture represented by a few preferred pathways.[1] These pathways are "paths of least resistance," where most of the flow goes (Tsang and Tsang, 1989), and are called flow channels by Neretrieks (1987) and others.

Over the last ten years or so, much work has been done in the area of fluid flow in heterogeneous fracture systems. This work, including both experimental observations and theoretical and modeling studies, is reviewed in the present paper. After a basic discussion of flow channeling in a single fracture, a comprehensive set of experiments in this field, from centimeter scale to kilometer scale, are described. Following that, we review the theoretical studies. We present the studies not so much in a historical sequence, but rather in a logical perspective. The paper concludes with a discussion of the implication of flow channeling in terms of predictive modeling for the study of nuclear or toxic waste isolation in geological formations.

Basic Description of Flow Channeling in a Fracture

To provide some general feeling for flow channeling, let us consider flow and tracer transport in a single fracture with variable aperture. The permeability k at any point on the fracture plane is assumed to be proportional to the square of aperture b at the point, which is strictly true for the permeability of a parallel-plate fracture with a

[1]The concept is different from the so-called flow fingering phenomenon in the petroleum literature, which arises from the interflow at the boundary of two fluids with different densities and viscosities. For example, when a fluid of high density and viscosity flows under gravity or pressure gradients towards a region of fluid with low density and viscosity, an instability of the two-fluid interface exists, and fingers of one fluid would be formed which flow into the other fluid as distinct, faster flow paths.

constant aperture b. Laboratory studies of core samples containing fractures (Gentier, 1986; Gale, 1987 and others) have shown that the variation of b over a fracture plane follows a log normal distribution:

$$n(b)db = \frac{1}{\sqrt{2\pi}\ln 10\sigma}\exp\left[-\frac{(\log b - \log b_0)^2}{2\sigma^2}\right]\frac{db}{b} \tag{1}$$

where n(b) db is probability of b, b_0 is the geometric mean of b values, and σ is the standard deviation of log b. In our calculation (Figure 1) the b values from the probability distribution are assigned onto a 40 × 40 grid using a geostatistical method. A number of geostatistical methods have been developed such as the COVAR code (Williams and El-Kadi, 1986), the 3-D Turning Band Random Field Generator (Tompson et al., 1989), and the geostatistical Library GSLIB (Deutsch and Journel, 1992).

The spatial distribution of the b values follows a covariance function. In the case of Figure 1, it follows an exponential function given by

$$E\left[(\log b(\bar{r}_1) - \log b_0)(\log b(\bar{r}_2) - \log b_0)\right] = \sigma^2 \exp\left[-\frac{2|r|}{\lambda}\right] \tag{2}$$

where E is the expectation value, $\bar{r}_1$ and $\bar{r}_2$ are the two spatial points where the b values are taken, and $|\bar{r}| = |\bar{r}_2 - \bar{r}_1|$ is the separation between the two points. The parameter λ is called the correlation length, which implies a correlation range of 3λ under the exponential form of spatial structure. One can extend this to the anisotropic case by defining λ_x, λ_y, and λ_z as associated with the Δx, Δy, and Δz components of $\bar{r}$ respectively, so that the right hand side of Equation (2) becomes

$$\sigma^2 \exp\left[-\frac{2\Delta x}{\lambda_x} - \frac{2\Delta y}{\lambda_y} - \frac{2\Delta z}{\lambda_z}\right] .$$

The 2-D distribution of aperture values generated in this way using the COVAR code (Moreno et al., 1990) is what is shown in the top part of Figure 1.

A high pressure is imposed on the left side of the flow domain and a lower one is applied on the right hand side, with the two remaining sides closed. Flow across the heterogeneous domain is then calculated by noting that the steady-state flow between two adjacent elements in the 40×40 mesh is given by Bird et al. (1960):

$$q_{ij} = \frac{1}{12\mu} b^3_m \cdot \Delta y \frac{p_i - p_j}{\Delta x} \tag{3}$$

where μ is liquid viscosity, p_i and p_j are pressures at elements, i and j, Δx and Δy are element lengths parallel and normal to flow respectively. The value b^3_m is the harmonic mean of the aperture values of the two elements

$$\frac{1}{b^3_m} = \frac{1}{2}\left(\frac{1}{b^3_i} + \frac{1}{b^3_j}\right) \tag{4}$$

For each element i without sources or sinks,

$$\sum_j q_{ij} = 0 \tag{5}$$

This system of Equations (3)–(5) are solved with the boundary conditions to yield all p_i, from which flow q_{ij} are then calculated. The results are shown in the lower part of Figure 1. Magnitudes of the fluid flow at any point are indicated by the widths of the flow lines (which is drawn as proportional to the square root of the flow rate). The figure shows that most of the flow follows two preferred paths even though no distinct path is noticeable in the permeability distribution (Figure 1, top). Flow channeling occurs in the heterogeneous system because, under a pressure gradient, flow seeks a few major paths of least resistance.

Now at a time designated as zero, a quantity of non-reactive solute, or tracer, is allowed to enter the fracture from the high-pressure boundary. It traverses the fracture plane and emerges on the low pressure side. The tracer concentration as it exists as a function of time is called the tracer breakthrough curve. Theoretically it can be

calculated using a particle tracking method (Moreno et al., 1990), by which a large number of particles (typically 10,000) are deposited at the left higher-pressure boundary at time zero and allowed to follow the streamlines to reach the low-pressure boundary on the right. The number of particles arriving at different time slots, between t and $t + \Delta t$, are plotted as a function of time. A typical result of the tracer breakthrough curve with the channeling effect is shown as a histogram in Figure 2.

Now, tracer transport in an aquifer is commonly described by a so-called advective dispersive equation, which for one dimensional flow has the form

$$\frac{\partial}{\partial x} D \frac{\partial C}{\partial x} - \frac{\partial}{\partial x}(Cv) = \frac{\partial C}{\partial t} \tag{6}$$

where C is the concentration, v is the pore velocity, and D is the dispersion coefficient. For a pulse release of particles, C_0 at $t = 0$ and $x = 0$, and under the boundary condition that at very large x the concentration and its derivative are zero, the equation has the solution (Robinson, 1984)

$$C_p(x,t) = \frac{C_0}{(4\pi Dt)^{1/2}} \exp\left(-\frac{(x - vt)^2}{4Dt}\right) \tag{7}$$

where $C_p(x,t)$ is the concentration (mass/length) at x and t. However, for the tracer breakthrough curve, we need the mass that has passed a boundary at s as a function of t. This is calculated from $C_p(x,t)$ as:

$$M_p(t) = \int_s^\infty C_p(x,t)dx = \frac{1}{2} C_0 \operatorname{erfc}\left(\frac{s - vt}{(4Dt)^{1/2}}\right) \quad . \tag{8}$$

The rate at which this mass passes a boundary $x = s$ is

$$R_p(t) = \frac{dM_p}{dt} \tag{9}$$

Then the mass collected at time t, between t and $t + \Delta t$ is given by

$$R_p(t)dt = \frac{C_0}{(4\pi Dt)^{1/2}} \exp\left(-\frac{(s-vt)^2}{4Dt}\right) \frac{s+vt}{2t} \Delta t \tag{10}$$

which is proportional to the concentration crossing the boundary x=s, since the flow rate is constant. This is a solution of the conventional advective dispersive equation, which allows two fitting parameters v and D. On Figure 2, we attempt to fit the numerical particle-tracking results of flow channeling with the conventional solution (Equation 10). Two fitting curves are presented by adjusting v and D values. It is apparent from the figure that the results of flow channeling cannot be fitted adequately, because of the presence of multiple peaks and long tail. These are characteristics of the flow channeling phenomenon.

Review of Experimental Observations

The experimental studies are reviewed in an order according to their scale. The first set of experiments are those performed on crystalline rock samples in the laboratory, with core diameter at the centimeter scale (Table 1). Pyrak-Nolte and co-workers (1987) studied a granitic core sample 5.2 cm in diameter, which had a fracture across its axis. They injected Wood's metal into the fracture from one side. After the metal solidified, the fracture was opened up to see the location of the Wood's metal residence. It is found that the Wood's metal occupied "preferred" portions of the fracture surface, and that its flow was highly non-uniform. Gentier used a larger core of medium-grained granite 12 cm in diameter, also with a natural fracture perpendicular to the core axis (Gentier, 1986; Gentier et al., 1989). A borehole was drilled in the middle of the core through which colored water was injected at the center of the fracture plane, and the emergence of the dyed water along the fracture trace on the circular surface of rock core was observed as a function of normal stress σ_N. It is shown that the dyed water does not emerge along the fracture trace evenly, but appears only at separated spots with a large difference in flow rates (Figure 3). Thus it can be inferred

that the water does not flow uniformly through the system but through channels. This effect was also observed in an experiment on a core with a fracture across its length (Neretnieks et al., 1982; Moreno et al., 1985), in which tracers flowed through the fracture over a distance of about 18 cm.

Hakami and Larsson (1996) made a detailed study of flow through a fracture, 41 cm long, parallel to the axis of a granitic core of 19-cm diameter. Experiments of flow over the length of the fracture were conducted as a function of normal stress across the fracture (from 0.03 to 1.2 MPa). These were then correlated to aperture distributions obtained by injecting fluorescent epoxy resin, letting it harden, and cutting the core into segments and measuring the aperture using a stereo-microscope. Based on these results, the authors studied the increase of the degree of flow channeling,with stress, and commented on the impact of fracture branching or intersection of one fracture with another.

The second set of experiments are field experiments at a small (2–30 m) scale (Table 2). Bourke (1987) and his coworkers selected several fractures in the Cornish granite in England and drilled five boreholes in the plane of one fracture with a length of about 2.5 m. Since the fracture plane undulates to a small extent, the five holes did not lie entirely in the fracture. Water was pressurized in one hole, and the adjacent holes were divided into 7-cm intervals by the use of packers, for measuring the pressure responses at different locations along these boreholes. It was found that many of the packed intervals in the five boreholes did not communicate with each other. Figure 4 shows a sketch of the connected flow pathways inferred from the measurements. As one can see, the flow areas occupy only about 20% of the fracture surface. This is mainly due to the fracture apertures not being uniform and the two fracture surfaces not being parallel plates. Rather, the aperture varies over the fracture plane, and pressurized water takes the easiest pathway from one drillhole to the other, resulting in channelized flow paths as shown.

A much more sophisticated and detailed field experiment at a similar scale was performed by Abelin and others (1988, 1990)—in the so-called "Channeling Experiment"—in which a fracture in granitic rock was selected in the Stripa iron mine in Central Sweden, 360 m below ground level. Two parallel boreholes were drilled in the fracture plane at 1.95 m apart. A specially designed packer system was used to inject five different tracers into 5-cm sections of one hole and observe their emergence in packered intervals in the other. Study of the results suggested a tracer transport pattern between the two boreholes shown in Figure 5, with breakthrough curves at different locations in the observation hole shown in Figure 6. Channelized flow was apparent, and the breakthrough curves showed multiple peaks and long tails.

The so-called "Stripa 2-D experiment" by Abelin and coworkers (1985) was a larger scale field experiment than the "Channeling Experiment." Two fractures in granitic rock were identified in one of the tunnels, or drifts, in Stripa Mine. A number of holes were drilled from the drift to intercept these fractures at points 5 to 10 m from the drift (Figure 7a). A tracer was deposited at the intersections bracketed by packers emplaced in these holes. The tracer flowed through the fracture plane towards the drift, emerging at the drift along the fracture trace on its ceiling and walls. The emergence of the tracer into the drift was not uniform along the fracture trace; rather, both the flow rate and the tracer concentration were highly variable (Figure 7b).

A further experiment was performed at a different location in the Stripa Mine, where a drift intersects a 6-m-wide fracture zone (Birgersson et al. 1993). This zone had a few very prominent flow paths, with the highest flowrate in one out of about 60 collection areas alone accounting for more than 50% of total flow.

The so-called "MI experiment" was carried out in a gneissose granodiorite rock mass at the Grimsel Underground Laboratory in Switzerland (Eikenberg et al., 1994; Frick et al., 1992; Hadermann and Heer, 1996) at a scale up to 20 m. In this experiment, a shear fault zone was identified to intercept the drift approximately normally. Eight

boreholes were drilled from the drift to intercept the fault zone at different points (Figure 8). Packers were placed in each borehole to bracket the interval at the fault zone, and pressure and tracer tests were performed to study the fault zone. Figure 9 shows an example of the breakthrough curves obtained by injecting tracer pulses at Well 86.004 and collecting samples at the Pumping Well 87.006, 4.9 m away (see Figure 8). Two different experiments were made with two different ratios of pumping to injection rates (β). The tracer breakthrough curves show features not normally associated with solutions of advective dispersive equations; namely, (a) the curves have a fast rise and long tail, and (b) sometimes these curves display multiple peaks. Such features were also seen in the "Channeling Experiment" (Abelin et al., 1990). As shown by the theoretical and modeling studies reviewed in the next section (and also Figure 1), these are the characteristics of flow channeling in heterogeneous systems.

Novakowski and coworkers (1985) conducted an experiment in a single fracture in a monzonitic gneiss rock body at Chalk River, Canada. They injected a pulse of conservative tracer in a steady state dipole flow field using an injection and a pumping well separated by 10.6 m. The tracer breakthrough curve did not display multiple peaks and they were able to fit it with a solution of the advective dispersive equation. This could be due to the integrative, hence smoothing, effect of a dipole flow field, so that at the pumping well where the tracer breakthrough data were collected, the tracer concentration represented the sum of tracer arrivals from a large number of streamlines.

Another set of five experiments were made in a single fracture in the same rock body (Raven et al., 1988) involving both injection-pumping dipole flow field and radial convergent flow field. Tracer transport distances ranged from 12.7–29.8 m. Raven et al. (1988) found that the breakthrough curves displayed long tails that could not be fitted by the advective dispersive equation. They obtained a much better fit when they assumed a "transient solute storage model" which includes a highly mobile flow path and adjacent stagnant or very slow water volumes with tracer exchange between them.

So far, the experiments discussed were all conducted on single fractures, which are essentially 2-D heterogeneous systems. On the next larger scale, one moves to multi-fracture systems (Table 3), beginning with the Stripa 3-D experiment. In this experiment, Neretnieks and coworkers examined a complex system, taken into account flow in three dimensions. Here, in a fractured granitic rock at Stripa Mine, a tunnel of about 100 m was isolated with three boreholes of 75 m in length, each drilled into the ceiling of the tunnel (Abelin et al., 1987). Nine high-transmissivity intervals were identified in the three boreholes from which different tracers were injected. The tunnel ceiling and walls were covered by 375 plastic rectangle sheets of 1 m × 2 m in dimension (Figure 10). The tracer emergence into the tunnel was studied by measuring and analyzing the flow into these plastic sheets. In Figure 10 it is seen that the tracer does not emerge uniformly over the whole tunnel surface, but rather at very selected locations. Both the flow rates and the tracer concentrations at different locations have a large degree of variability.

Another 3-dimensional tracer test was performed in the Fanay Augeres uranium mine, France, and reported by Calmels et al. (1986) and Barbreau et al. (1987) to study the scale effect of flow and transport in fractured rocks. This is a densely fractured granitic rock site, with fracture spacing on the order of 10 cm. However, spacings between larger-size fractures are much larger. A drift of about 100 m long was used, and three sets of three 50-m-long boreholes were drilled radially into granitic rock from the drift (Figure 11). Boreholes F2 and F3 (see Figure 11) were packered off in 5-m sections through which tracers were injected. Tracer arrival was measured in the drift at three locations: (A) the area under the injection borehole; (B) the area at 0–25 m downstream from the injection section; and (C) the area 25–50 m downstream. Note that the tracer collection or observation is not at localized "point" locations, but each covers a portion of the drift 25 m in length for both Cases B and C. Examples of the breakthrough curves are shown in Figure 12. They do not show multiple peaks,

probably due to the integrative or smoothing effect of tracer collection over a drift section of 25 m which is 250 times the fracture spacing. Among the four curves in Figure 12, one (lower right curve) can be matched by the conventional solution of advective dispersive equation, while the others all display the fast-rise and long-tail behavior typical of channeling flow.

Field experiments at a scale of 100 m or more were conducted at the Finnsjön site in Sweden and at the Underground Research Laboratory in Whiteshell, Canada. At the Finnsjön site (Andersson et al., 1988; 1989; 1990), two fracture zones were identified in a granodioritic formation. The deeper one, Zone 2, with a thickness of about 200 m located at 100–260 m below the ground surface, was chosen for tracer experiments. A number of injection and withdrawal wells were drilled into the fracture zone (Figure 13), and a large number of tracers were used to study tracer transport between wells at the distance of 150–200 m. A typical breakthrough curve is shown in Figure 14 for the case of a tracer pulse released in Well KFi06 and collected at the Pumping Well BFi02 (see Figure 13). The latter well has a constant pumping rate and established a convergent flow field for tracer transport. Again, behavior typical of channeling flow is observed for the breakthrough curve, which displays a long tail and one major peak at 400 hours and two minor peaks at 950 and 1400 hours respectively.

The other large scale tracer experiments were carried out by Davison and coworkers at the Underground Research Laboratory (URL) at Whiteshell, Canada (Thompson and Simmons, 1995). At that site, three fracture zones were identified in the granitic Lac du Bonnet batholith. Tracer tests were conducted in the upper two, labelled FZ2 and FZ3 (Figure 15; Frost et al., 1992 and Frost and Davison, 1994). The fracture zone FZ2 has a "branch-off" labelled FZ2-splay in Figure 15. In two-well injection-withdrawal tests in FZ2, multiple peaks were observed in tracer breakthrough curves at short transport distances (about 20 m); while for large transport distances, a single well-dispersed peak was obtained (Frost et al., 1992). For the tests in FZ3, the

tracers were injected in wells in the radially converging groundwater flow field surrounding the URL shafts and collected at groundwater seepage locations in the main and ventilation shafts of the URL. Of the more than 30 breakthrough curves obtained, twelve display multiple peak behavior, and many have early sharp rise and long tail features, both of which indicate the possible effects of flow channeling. Examples are shown in Figure 16.

Large-scale observations in drifts and tunnels have also shown the clear effects of channeling flow. At the so-called SFR site at Forsmark, which hosts the Swedish repository for low and intermediate level radioactive waste, more than 14 000 m^2 of tunnel wall surfaces were surveyed for water effluent spots, and their widths and flow rates were measured. The sparse locations where the water flow emerged in the tunnel and silo system are shown in Figure 17 (Neretnieks, 1994). Measured flow rates are indicated by the length of straight lines at different locations, as shown in Figure 17. Strong variability is found. A special survey was also conducted at Kymmen, another Swedish site, along a 4.5-km-long full-face drilled tunnel in crystalline rocks. A large number of spots or channels with flowing water were charted and used to evaluate the widths, average channel densities and lengths, as well as the standard deviation in flow rate distribution (Moreno and Neretnieks, 1993). At the SFR site, one spot per 35 m^2 was estimated, while in the Kymmen tunnel, there was one spot every 105 m^2 in the "good rock" and one spot per 21 m^2 in the fracture zones.

The above experiments are listed and summarized in Tables 1, 2, and 3. A number of ongoing field experiments at Kamaishi, Japan (Sawada et al., 1996; Uchida et al., 1996); Aspo, Sweden (Bäckblom, 1995; Winberg, 1996); and WIPP site, USA (Jones et al., 1992; Beauheim et al., 1995), are also indicated at the end of Table 3. Important new results on flow and transport in fractured rock can be expected from these field studies in the near future. Overall, one can see that flow channeling is a prevailing phenomenon at all scales in fractured rocks. The channeling phenomenon

observed in small scale experiments in the laboratory and in single fracture experiments in the field may be due to the heterogeneity of the aperture in the fracture plane. However, for three-dimensional experiments in the field, flow channeling may also be due to variability in fractures and porous medium transmissivity distributions. These experiments have stimulated a large amount of theoretical and modeling studies, which will be reviewed in the next section.

Review of Theoretical and Modeling Studies

Because of their observations in experiments in the Stripa mine, Neretnieks and coworkers have developed a concept that flow in the fractured rocks must be through channels; their work on flow through one or multiple channels in parallel were presented in Rasmuson and Neretnieks (1986) and Neretnieks (1987). In some cases these channels are assumed to be separate, while in other cases they communicate with each other. Tsang and Tsang (1987) extended the model of uniform channels to that of channels with variable apertures along their lengths, and used a numerical stochastic approach to study their properties.

Tsang and Tsang (1989) pointed out that these channels are not physical or geometric channels in the fracture plane. They showed that for a 2-dimensional heterogeneous system with a hydraulic potential gradient across it, flow will search through the heterogeneous plane for the least resistant paths (Figure 1). Thus, a potential gradient applied across the fracture from different directions (top to bottom or left to right in Figure 1) will yield sets of "channels" very different from each other in geometry. Furthermore, they showed that these different sets of channels nevertheless have the same statistical properties (Figure 18); i.e., they can be characterized by the same mean and standard deviation values for the probability distribution function of permeability. The channels are therefore more like the stream-tubes in potential theory rather than discrete geometric features in a single fracture.

Moreno and Tsang (1994) extended the studies from two to three dimensions. They generated a 3-dimensional stochastic heterogeneous system based on the mean and standard direction of the permeability probability distribution together with a spatial correlation length. Looking at the 3-dimensional heterogeneous block where all the permeability variations are embedded, no discrete flow path can be identified. However, by applying a potential gradient through the system, channeling occurs as a function of the degree of variability or standard deviation for the distribution of permeability. This channeling effect is clearly illustrated in Figure 19 as least-resistive flow paths. Following Tsang and Tsang (1989), they confirmed that channels generated by different potential gradient directions have the same statistical parameters, which differ from those of the 3-dimensional permeability distribution. An interesting result shown in Figure 20 is the breakthrough curves of tracer arrival at the low-pressure side of a heterogeneous block, due to a tracer pulse released from the opposite high-pressure side. These curves are calculated for different variances of the permeability values, and they are normalized with respect to the mean arrival time. At low variance or standard deviation (natural log permeability $\sigma < 1$), a typical solution of the advective dispersive equation is found. However, as σ increases, a new peak appears at an early time, representing a "fast" path, and the curve has the characteristic fast-rise and long-tail features. It is interesting to note that these flow channeling results of Moreno and Tsang (1994) are valid for both small and large-scale systems, so long as they are strongly heterogeneous and have spatial correlation lengths comparable to the dimension of the flow domain (say 0.05–0.3). These systems could well be a network of many fractures.

The two-dimensional channeling flow in heterogeneous fracture systems were also studied by Moreno et al. (1988, 1990) and Tsang et al. (1988), who conducted comprehensive model studies on flow and transport as a function of mean and standard deviation of permeability and spatial correlation lengths. It is interesting that the

authors demonstrated that the spatial correlation length, λ, is not a critical parameter in the behavior of flow channeling, so long as it is of a reasonable value, namely, $0.05 < \lambda/L < 0.3$ approximately, where L is the tracer transport distance. Various "anomalous" behaviors that one would expect in experimental observations due to flow channeling effects were also discussed.

The concept of flow channeling in heterogeneous systems has been incorporated in the understanding and model analysis of field data. Moreno and Tsang (1991) did calculations stimulated by the MI experiment at Grimsel, where it was seen that the tracer transport from one well to another in a two-dimensional heterogeneous fracture zone displayed double peaks in the breakthrough curves (see Figure 9). Moreno and Tsang were able to demonstrate in their model study that such double peaks occur because of multiple flow channels through the system. In particular, the relative height of the double peaks may vary with injection rates, which is unexpected behavior for homogeneous flow systems but was observed in the MI experiment. This is shown in Figures 21 and 22. In these figures, a well is located at the upper right corner, pumping at a rate Q, and tracer is released at a point in the 2-D heterogeneous plane with an injection rate $q << Q$. The variation of q/Q causes the tracer to seek alternative flow paths.

The Stripa-3D experimental data by Neretnieks and coworkers (Abelin et al., 1987) were studied and analyzed by Tsang et al. (1991) using the simplified flow channeling model (Figure 23), based on the results of various detailed theoretical studies on flow channeling. Thus, in analyzing tracer transport in fractured media, this model assumes that such transport is by way of one or more one-dimensional tortuous channels, each with variable aperture along its length. These channels correspond to one or more peaks in the breakthrough curves. In the case of Stripa-3D experiment, because the experimental tracer injection rate varied strongly, a deconvolution method, called the Toeplitz Analysis method, was developed and applied to the data to obtain

the equivalent breakthrough curves for tracer injected as an instantaneous pulse. Multiple channels in the flow systems were found in the form of distinct peaks in the equivalent breakthrough curves for pulse injection (Figure 24). A similar approach was taken by Ilvonen et al. (1994) to study the Stripa-3D data, including a careful sensitivity analysis. They pointed out that great care is needed in interpreting such data. Hodgkinson and Grindrod (1991) also studied the data and determined the flow dimension using a continuous-dimension analysis concept which allows fractional dimension between 1 and 3 (Barker, 1985, 1988). A flow dimension of 1 would indicate a linear flow pattern; a dimension close to 2 would indicate the presence of cylindrically radial flow pattern in an approximate fracture plane, while a dimension close to 3 would indicate a spherically radial flow pattern within a highly fractured domain. Their analysis showed that the average flow dimension is 1.11, indicating a linear or channelized flow pattern. Hautojärvi and Taivassalo (1994), and Goblet (1992), have independently analyzed the tracer test data from Finnsjön (Andersson et al., 1990) using a multiple-channel model. They were able to explain the overall features of both the radial convergent and the dipole tracer tests at Finnsjön with similar channel parameters, thus providing confidence in the flow-channeling model.

The incorporation of flow channeling in three-dimensional fracture network models has also been approached by a number of authors. Cacas and coworkers (1990) developed a network model in three dimensions in which they assumed that the flow from fracture to fracture in the fracture network system is by way of channels of rectangular cross sections (Figure 25). The model has been applied to the tracer transport experiment in granitic fractured rock at Fanay-Augères Mine, France (Calmels et al., 1986). They showed that the fracture network model of channels gives a distribution of possible transport times and a distribution of the width values around the peaks in breakthrough curves. The experimental observations were used to calibrate the model to obtain the optimal stochastic parameters. One important point

from this paper is that because of heterogeneity, the results from the model has to be given in terms of distributions rather than in simple predictive values. Figure 26 gives an example of such distributions for model predictions. Here, the arrival time of a peak in the tracer breakthrough curve was calculated. Because the fracture-channel network model is stochastic, based on specified mean and standard deviation parameters for network properties, a number of equally likely realizations of the model can be generated. In this figure, peak arrival times calculated for a large number of realizations for four transport distances (corresponding to the Fanay-Augeres experiment) were presented as a histogram of probabilities. These can be compared with experimental observations (indicated by stars, one each in the four subgraphs).

Nordqvist and coworkers (1992) developed a 3-dimensional fracture network model with flow channeling within each fracture. They assumed that relatively large permeabilities exist at fracture-fracture intersections, and consequently the pressure along the length of an intersection is constant (though they might be different from intersection to intersection). Given that approximation, the flow channeling can be solved within each fracture independently and then incorporated in the 3-dimensional fracture network system. This approach is illustrated in Figure 27. The right hand side of the figure shows a single fracture being defined in terms of its aperture b_0 and the aperture standard deviation σ_b, based on which multiple realizations of its hydraulic conductivity τ_i and tracer travel times $g_i(t)$ are calculated. These are imported to each fracture in the network shown on the left side of Figure 27 by a random selection for each model realization. Application of this model to the calculation of tracer breakthrough curves yields all the features in the results from field experiments; i.e., fast rise, long tail, and the multiple peaks, as a function of transport distance (Figure 28). They noted that multiple peaks should be expected for shorter tracer transport distances (distances comparable to the fracture spacing), while at a larger distance, a single wide peak may emerge. This corresponds to the analysis results of the tracer

tests in the Fracture Zone 2 at the Canada URL reported by Frost et al. (1992). The approach of Nordqvist et al. was also applied to study the effective transmissivity and adsorption in fractured rocks at multiple scales (Nordqvist et al., 1996).

Moreno and Neretnieks (1993) in their channeling model took a similar approach as that of Cacas et al. (1990), but from a different starting point. They based their model on observations that when two fracture planes intersect, a channel in one fracture can intersect the channel in another fracture, forming a cross with four channel members intersecting. In addition, if the line along the fracture intersection has a relatively large permeability, as was observed in the Stripa-3D experiments (Abelin, et al., 1987) and in field observations at Forsmark and the Kymmen tunnel in Sweden (Neretnieks, 1994), two further channel members can intersect in the same point, making a total of six channel members intersecting at one point. A three-dimensional channel network can then be formed, and each channel member is assigned a conductance, length and volume. This is sufficient to fully determine the flowrate distribution and water residence time distribution (RTD) in the network. If the matrix diffusion and sorption properties are known, the RTD of solutes that can diffuse into the rock matrix and be sorbed there can also be assessed. For the sorbing solutes, the influence of channel volume on RTD is often negligible and need not be known. The most important data for the model can be estimated from hydraulic tests in boreholes. To obtain data on channel widths and lengths, observations in drifts and tunnels were used. Because the model uses hydraulic information to obtain data for the conducting "channel members," it does not need detailed measurements on fracture orientations and fracture lengths as fracture network models do. One special strength of the model is that it can handle matrix diffusion with ease. The model has been used to interpret field tracer tests at Stripa, and recently also those in the Hard Rock Laboratory at Aspö in Sweden (Neretnieks, 1994).

Finally, Tsang and coworkers (Tsang and Tsang, 1993; Tsang et al., 1996) developed a stochastic continuum model of heterogeneous fractured rocks by assuming that the porous matrix is permeable as well as the fractures in the medium. They used the method of Góméz-Hernández and Srivastava (1990), and developed a stochastic model, in which the three-dimensional heterogeneous porous medium contains fractures represented by a relatively higher density of large permeability values along prescribed orientations. Thus, within the same stochastic continuum model with a specified distribution of permeabilities, they are able to construct a consistent fractured porous medium. Pressure gradients were applied across the model domain, and the preferred channels were calculated. On the exit surface where the tracer is observed, strong variability is seen from point to point (Figure 29). Tsang and Tsang proposed that averaging the tracer breakthrough data over the surfaces is needed in order to study the overall effect of flow through fractured porous medium systems. Further, they pointed out the need to perform multiple tracer tests at different locations in the 3-D block in order to be able to characterize its stochastic properties for transport modeling (Figure 30).

From the review of theoretical and modeling studies presented above, it can be seen that flow channeling in heterogeneous systems can be studied and its properties evaluated, in both 2-D and 3-D systems. The direction of further work is first, to understand its impact on parameters usually associated with geologic formations in the homogeneous model, such as effective permeability, dispersivity and sorption coefficients; and second to address the critical question of how to make predictions of solute travel times in the geosphere, where flow channeling will almost certainly occur to some degree.

Concluding Remarks on Flow Channeling and Its Implication in Practical Problems

Experimental observations and theoretical work have demonstrated that flow channeling is a common phenomenon in nature. The reason it has come to the forefront of recent scientific investigations is the current interest in predicting solute transport in a geological medium that is much more sensitive to medium heterogeneity than temperature or pressure fields. The experimental work has shown that such an effect occurs on all scales, from centimeter to kilometer scale. The theoretical work has also demonstrated this phenomenon through numerical stochastic modeling techniques. They have provided a basic understanding of the occurrence of such features and attempted to determine the characteristic properties of the channels relative to properties of the heterogeneous system as a whole.

In this paper, we have emphasized that the flow channeling phenomenon gives rise to a fast rise and long tail in breakthrough curves. However, other mechanisms may also contribute to the observation of long tails in some cases. One such mechanism is that the solutes diffuse in and out of stagnant or near stagnant waters in the system. The largest stagnant water body, by far, is that in the porous matrix of the rock. This effect can be very strong, especially for experiments with durations of several days or more. Hence, it is difficult to use the tail ends of breakthrough curves alone to assess channeling properties.

It has also been pointed out (Olsson, 1992) that observations on drifts and tunnels can be influenced by degassing of the water as it flows to a region near the drift from the interior of the rock and the pressure drops. The gas that evolves from its solution in water may clog the more open parts of the fracture and reduce its permeability. This effect may be especially noticeable at larger depths, where the water under pressure can contain higher concentrations of dissolved gases.

In modeling a specific field site, discrete features of large-scale heterogeneities should be measured and modeled deterministically. Even after these large features are accounted for, there remain significant heterogeneities that give rise to flow channeling, the subject of this review. Theoretical studies on flow channeling have been used to understand specific experiments such as the Stripa 3-D experiment and Finnsjön experiment. However, it is difficult to predict the channeling flow locations and channeling breakthrough curves. This is an important problem because the current interest in isolation properties of geological systems for nuclear and toxic waste isolation requires some degree of predictive capability on solute transport. In Cacas' approach (Cacas et al., 1990), the prediction of flow and transport was given in terms of probability distributions of travel times and travel time dispersion values. Thus, it is not possible to predict a unique travel time many years into the future, but rather a probability distribution of travel times. Tsang and Tsang (1993) proposed an approach based on the view that, though we might not be able to predict the tracer breakthrough curves at a specific location in the observation domain because of its variation within this domain, we may yet take the average of the tracer breakthrough curves over a large domain. They have demonstrated that if the averaging domain is larger than heterogeneity spatial scale, the results are much more stable and independent of detailed variability. This means that the predictive quantities required for transport processes in a geologic system thousands of years into the future must be spatially averaged. This has practical implications, not only in terms of the regulatory requirements involving such predictive quantities, but also in terms of what data are needed for this kind of model in order for making predictions. Currently, measurements of permeability and porosity are made by means of well testing or local tracer tests, but it is not clear that such measurements are sufficient. Because of the variability of the properties of the heterogeneous system, Tsang and Tsang (1993) advocate that a number of such experiments at alternative locations are needed in order

to obtain the appropriate statistical properties for making correct predictions. There is then a close coupling between data needs and predictive quantities, so that it is no longer a two-step process in which one obtains the data and then makes the predictions, but rather the two are highly coupled and iterative (Tsang et al., 1994). These unanswered questions suggest directions for future research.

Acknowledgments

The paper is prepared with the joint support of Nuclear Power and Fuel Development Corporation (PNC), Japan, and Office of Energy Research, Office of Basic Energy Sciences, Engineering and Geosciences Division, of the U.S. Department of Energy under Contract No. DE-AC03-76SF00098. The second author, Neretnieks, thanks the Swedish Nuclear Waste Management Company (SKB) who have supported his involvement in the various investigations in the Stripa Mine and other projects. Review and very helpful comments by John Apps and Chao Shan, and by three anonymous reviewers and James A. Smith, Editor of Review of Geophysics, are gratefully acknowledged.

References

Abelin, H., I. Neretnieks, S. Tunbrant, and L. Moreno (1985). Final Report of the Migration in a Single Fracture, Experimental Results and Evaluation, *Stripa Project, Tech. Rep. 85-103*, Nucl. Field Safety Proj., Stockholm, Sweden.

Abelin, H., L. Birgersson, H. Wilén, T. Ågren, L. Moreno, and I. Neretnieks (1990). Channeling experiment, *Stripa Project, Tech. Rep. 90-13*, Nucl. Fuel Safety Proj., Stockholm, Sweden.

Abelin, H., L. Birgersson, J. Gidlund, L. Moreno, T. Agren, H. Widen, and I. Neretnieks (1987). 3-D Migration Experiment in Sparsely Fractured Crystalline Rock, *Proc. Sci. Basis Nucl. Waste Manag. XI*, Boston MA, edited by M.J. Apted and R.F. Westerman, Mat. Res. Soc., v. 112, pp. 199–207 (see also *Stripa Project, Tech. Rep. 87-21*, Nuclear Fuel Safety Proj., SKB., Stockholm, Sweden).

Abelin, H., L. Birgersson, T. Agren, and I. Neretnieks (1988). A Channeling Experiment to Study Flow and Transport in Natural Fractures, *Proc. Sci. Basis Nucl. Waste Manag. XII*, Berlin, Germany, edited by L. Lutze and R.C. Ewing, Mat. Res. Soc., V. 127, pp. 661–668.

Andersson, J-E, L. Ekman, E. Gustafsson, R. Nordqvist, and S. Tiren (1989). Hydraulic interference tests and tracer test within the Brändan Area, Finnsjön study site. The fracture zone project phase 3. Swedish Nuclear Fuel and Waste Management Company, SKB progress report 89-12.

Andersson, J-E., L. Ekman, and A. Winberg (1988). Detailed investigations of fracture zones in the Brändan Area, Finnsjön study site. Single hole water injection tests in detailed sections. Analysis of conductive fracture frequency. Swedish Nuclear Fuel and Waste Management Company, SKB progress report 88-08.

Andersson, J., and B. Dverstorp (1987). Conditional Simulations of Fluid Flow in Three-Dimensional Networks of Discrete Fractures, *Water Resources Research*, 23(10), 1876–1886.

Andersson, P., C.O. Eriksson, E. Gustafsson, and T. Ittner (1990). Dipole tracer experiment in a low-angle fracture zone at the Finnsjön site, Central Sweden—Experimental design and preliminary results. Swedish Nuclear Fuel and Waste Management Company, SKB progress report 90-24.

Bäckblom, G. (1995). The Rôle of the Äspö Hard Rock Laboratory in the Swedish Deep Repository Programme. *Proceedings of the Sixth Annual International Conference on High Level Radioactive Waste Management*, Las Vegas, Nevada, April 30–May 5, 1995, pp. 175–177.

Barbreau, A., M.C. Cacas, E. Durand, B. Feuga (1987). Hydrodynamic Characterization of a Fractured Granite Body at Various Scales, in *Proceedings, International Society for Rock Mechanics*, 6th International Congress on Rock Mechanics, Montreal, Canada, Aug. 30–Sept. 3, 1987, pp. 15–22.

Barker, J.A. (1985). Block geometry function characterizing transport in densely fissured media, *J. of Hydrology*, 77, 263–279.

Barker, J.A. (1988). A Generalized Radial Flow Model for Hydraulic Tests in Fractured Rock, *Water Resour. Res.*, 24(10), 1796–1804.

Bear, J., C.F. Tsang, and G. De Marsily (editors), 1993. Flow and Contaminated Transport in Fractured Rock, Academic Press, San Diego.

Beauheim, R.L., L.C. Meigs, G.J. Saulnier, and W.A. Stensrud (1995). Culebra Transport Program Test Plan: Tracer Testing of the Culebra Dolomite Member of the Rustler Formation at the H-19 and H-11 Hydropads on the WIPP Site. Sandia National Laboratories.

Bird, R.B., W.E. Stewart, and E.N. Lightfoot (1960). *Transport Phenomena*, John Wiley, New York.

Birgersson, L., L. Moreno, I. Neretnieks, H. Widen, and T. Igren (1993). A Tracer Experiment in a Small Fracture Zone in Granite, *Water Resources Research* ,Vol. 29, no. 12, p 3867–3878.

Bourke, P.J. (1987). Channeling of Flow Through Fractures in Rock, *Proceedings of GEOVAL-87 International Symposium*, Swedish Nuclear Power Inspectorate (SKI), Stockholm, Sweden, April 7–9.

Cacas, M.C., E. Ledoux, G. deMarsily, A. Barbreau, P. Calmels, B. Gaillard, and R. Margrita (1990). Modeling Fracture Flow with a Stochastic Discrete Fracture Network: Calibration and Validation, 2. The Transport Model, *Water Resources Research*, V. 26, No. 3, 491–500.

Calmels, P., B. Gaillard, R. Margrita (1986). "Etude de l'Effet d'Echelle en Milieu Fissuré – Phase 2B: Etude des Migrations, Essais de Tracages," Volumes A et B – Centre d'Etudes Nucléaires de Grenoble, Office des Rayonnements Ionisants – Grenoble – Ref: ORIS/DAMRI/SAR/SAT/RAP/86-14/PCs.

Dershowitz, W.S., and T.S. Schrauf (1987). Discrete Fracture Flow Modeling with the JINX Package, *Proc. 28th Symp. Rock Mech.*, Tucson, AZ, edited by I.W. Farmer, J.J.K. Daemen, C.S. Desai, C.E. Glass, and S.P. Neuman, pp. 433–440.

Deutsch, C.V. and A.G. Journel (1992). GSLIB–Geostatistical Software Library and User's Guide, Oxford University Press, New York, Oxford.

Dverstorp, B., and J. Andersson (1989). Application of the Discrete Fracture Network Concept with Field Data: Possibilities of Model Calibration and Validation, *Water Resour. Res.*, Vol. 25, No. 3, p. 540–550.

Eikenberg, J., E. Hoehn, Th. Fierz, and U. Frick (1994). Grimsel Test Site: Preparation and Performance of Migration Experiments with Radio Isotopes of Sodium, Strontium and Iodine, Paul Scherrer Institut Report, PSI Bericht Nr.94-11.

Endo, H.K., J.C.S. Long, C.R. Wilson, and P.A. Witherspoon (1984). A Model for Investigating Mechanical Transport in Fracture Networks, *Water Resour. Res.*, Vol. 20,No. 10, p. 1390–1400.

Frick, U., W.R. Alexander, B. Baeyens, P. Bossart, M.H. Bradbury, Ch. Bühler, J. Eikenberg, Th. Fierz, W. Heer, E. Hoehn, I.G. McKinley, and P.A. Smith (1992). Grimsel Test Site: The Radionuclide Migration Experiment—Overview of Investigations 1985–1990, Paul Scherrer Institute Report, PSI Bericht Nr. 120.

Frost, L.H. and C.C. Davison (1994). Summary of the Fracture Zone 3 Groundwater Tracer Test Program at the Underground Research Laboratory, Applied Geoscience Branch, Whiteshell Laboratories, Pinawa, Manitoba R0E 1L0, Report TR-617.

Frost, L.H., N.W. Scheier, E.T. Kozak, and C.C. Davison (1992). Solute transport properties of a major fracture zone in granite, in *Tracer Hydrology*, Hötzl and Werner (eds.), Balkema Publishers, Rotterdam, pp. 313–320.

Gale, J.E.(1987). Comparison of Coupled Fracture Deformation and Fluid Flow Models with Direct Measurements of Fracture Pore Structure and Stress-Flow Properties, *Proceedings of the 28th U.S. Symposium of Rock Mechanics*, Tucson, Arizona p. 1213–1222.

Gentier, S. (1986). Morphologie et Comportement Hydromécaique d'une Fracture Nauturelle dans un granite sous Contrainte Normale: É tude Expérimentale et théorique Ph.D. Thése, Vol. 1 and Vol. 2, Universite d'Orléans.

Gentier, S., D. Billaux, and L. van Vliet (1989). Laboratory Testing of the Voids of a Fracture, *Rock Mech. Rock Eng.*, Vol. 22, No. 2, p. 149–157.

Goblet, P. (1992). EMP Analysis of Tracer Data, in Studies of Tracer Experiments in a Fracture Zone at the Finnsjön Research Area, C.-F. Tsang and S. Neuman, eds., *Report of the International INTRAVAL Project, Phase 1*, Swedish Nuclear Power Inspectorate (SKI) and Nuclear Energy Agency, OECD.

Góméz-Hernández, J.J., and R.M. Srivastava (1990). ISIM3d: An ANSI-C three-dimensional multiple indicator conditional simulation program, *Comput. Geosci.*, Vol. 16, No. 4, p395–440.

Hadermann, J. and W. Heer (1996). The Grimsel (Switzerland) Migration Experiment—Integrating Field Experiments, Laboratory Investigations and Modelling, *Journal of Contaminant Hydrology*, Vol. 21, No. 1-4, pp. 87–100.

Hakami, E. and E. Larsson (1996). Aperture Measurements and Flow Experiments on a single Natural Fracture, *International Journal of Rock Mechanics and Mining Sciences and Geomechanics Abstracts*, Vol. 33, No. 4, pp. 395–404.

Hautojärvi, A., and V. Taivassalo (1994). The INTRAVAL Project—Analysis of the Tracer Experiments at Finnsjön by the VTT/TVO Project Team, Nuclear Waste Commission of Finnish Power Companies, Report YJT-94-24.

Hodgkinson, D., and P. Grindrod (eds.) (1991). The International Intraval Project. Phase 1, test case 4. Flow and tracer experiment in crystalline rock based on the Stripa 3-D experiment. SKI and OECD/NEA, Paris.

Ilvonen, M., A. Hautojärvi, and P. Paatero (1994). Analysis of Stripa 3D Data by a Deconvolution Technique, Nuclear Waste Commission of Finnish Power Companies, Report YJT-94-14.

Javadel, I., C. Doughty, and C.F. Tsang (1984), Groundwater Transport, Water Resources Monograph 10, American Geophysical Union, Washington D.C.

Jones, T.L., V.A. Kelley, J.F. Pickens, D.T. Upton, R.L. Beauheim, and P.B. Davies (1992). Integration of Interpretation Results of Tracer Tests Performed in the Culebra Dolomite at the Waste Isolation Pilot Plant Site, Sandia National Laboratories Report SAND92-1579.

Kobus, H., B. Barczewski and H. Koschitzky, editors (1996). *Groundwater and Subsurface Remediation*, Springer Verlag, Berlin, Heidelberg.

Long, J.C.S., J.S. Remer, C.R. Wilson, and P.A. Witherspoon (1982). Porous Media Equivalents for Networks of Discontinuous Fractures, *Water Resour. Res.*, Vol. 18, No. 3, p. 645–658.

Moreno, L. and C.-F. Tsang (1991). Multiple-Peak Response to Tracer Injection Tests in Single Fractures: A Numerical Study, *Water Resour. Res.*, Vol. 27, No. 8, p. 2143–2150.

Moreno, L. and C.-F. Tsang (1994). Flow Channeling in Strongly Heterogeneous Porous Media: A Numerical Study, *Water Resources Research*, Vol. 30, No. 5, p. 1421–1430.

Moreno, L. and I. Neretnieks (1993). Fluid Flow and Solute Transport in a Network of Fractures. *J. of Contaminant Hydrology*,, Vol. 14, p. 163–192.

Moreno, L., I. Neretnieks, and T. Eriksen (1985). Analysis of Some Laboratory Tracer Runs in Natural Fissues, *Water Resour. Res.*, Vol. 21, No. 7, p. 951–958.

Moreno, L., Y.W. Tsang, and C.-F. Tsang (1990). Some Anomalous Features of Flow and Solute Transport Arising from Fracture Aperture Variability, *Water Resour. Res.* 26, No. 10, p. 2377–2391.

Moreno, L., Y.W. Tsang, C.-F. Tsang, F.V. Hale, and I. Neretnieks (1988). Flow and Tracer Transport in a Single Fracture: A Stochastic Model and Its Relation to Some Field Observations, *Wat. Resour. Res.* Vol. 24, p. 2033–2048.

National Research Council (1996). *Rock Fractures and Fluid Flow*, National Academy Press, Washington, D.C.

National Research Council (1984). *Groundwater Contamination*, National Academy Press, Washington, D.C.

Neretnieks I. (1994). Nuclear Waste Repositories in Crystalline Rock—An Overview of Nuclide Transport Mechanisms. *Proceedings of the MRS Meeting on Scientific Basis for Nuclear Waste Management*, Kyoto, Japan, Oct. 24–26, pp. 7–20.

Neretnieks, I. (1987). Channeling Effects in Flow and Transport in Fractured Rocks—Some Recent Observations and Models, *Proceedings of GEOVAL Symposium*, Swedish Nuclear Power Inspectorate (SKI), Stockholm, p. 315–335.

Neretnieks, I., T. Eriksen, and P. Tähtinen (1982). Tracer Movement in a Single Fissure in Granitic Rock: Some Experimental Results and their Interpretation, *Wat. Resour. Res.*, Vol. 18, p. 849–858.

Nordqvist, A.W., Y.W. Tsang, C.F. Tsang, B. Dverstorp, and J. Anderson (1996). Effects of High Variance of Fracture Transmissivity on Transport and Sorption at Different Scales in a Discrete Model for Fractured Rocks, *Journal of Contaminant Hydrology*, Vol. 22, No. 1–2, pp. 39–66.

Nordqvist, A.W., Y.W. Tsang, C.F. Tsang, B. Dverstorp, and J. Andersson (1992). A Variable Aperture Fracture Network Model for Flow and Transport in Fractured Rocks, *Water Resour. Res.*, Vol. 28, No. 6, p. 1703–1713.

Novakowski, K.S., G.V. Evans, D.A. Lever, and K.g. Raven (1985). A Field Example of Measuring Hydrodynamic Dispersion in a Single Fracture, *Water Resources Research* Vol. 24, No. 8, p. 1165–1174.

Nuclear Energy Agency (1996). Update in Waste Management Policies and Programmes, *Nuclear Waste Bulletin*, OECD, Paris.

Olsson, O. (ed.) (1992). Stripa Project, Site Characterization and Validation—Final Report, *SKB Technical Report 92-22*, Swedish Nuclear fuel and Waste Management Company, (SKB), Stockholm, Sweden.

Pyrak-Nolte, L.J., L. Myer, N.W. Cook, and P.A. Witherspoon (1987). Hydraulic and mechanical properties of natureal fractures in low permeability rock. *Proceedings of the Sixth International Congress for Rock Mechanics*, Montreal, Canada, Aug. 30 to Sept. 3, 1987, pp. 225–231.

Rasmuson, A., and I. Neretnieks (1986). Radionuclide Transport in Fast Channels in Crystalline Rock, *Water Resources Res.*, Vol. 22, p. 1247–1256.

Ravin, K.G., K.S. Novakowski, and P.A. Lapcevic (1988). Interpretation of Field Tracer Tests of a Single Fracture Using a Transient Solute Storage Model, *Water Resources Research*, Vol. 24, No. 12, pp. 2019–2032.

Robinson, P.C., (1984). Connectivity, Flow and Transport in Network Models of Fractures Media, Ph.D. thesis, Oxford University, Oxford, 1984.

Sawada, A., M. Uchida, T. Senba, M. Shimo, and T. Doe, (1996). A characterization of conductive fractures using pressure interference observation during borehole drilling, *Proc. of the 27th JSCE Symposium of Rock Mechanics*, p. 176–180 (in Japanese with English abstract).

Thompson, A.F.B., R. Ababou, and L.W. Gelhar (1989). Implementation of the Three-Dimensional Turning Bands Random Field Generator, *Water Resour. Res.*, Vol. 25, No. 10), pp. 2227.

Thompson, P. and G. Simmons (1995). Underground Laboratories—A Site Characterization Tool for Nuclear Fuel Waste Disposal in Canada. *Proceedings of the Sixth Annual International Conference on High Level Radioactive Waste Management*, Las Vegas, Nevada, April 30–May 5, 1995, pp. 169–171.

Tsang, C.-F., L. Gelhar, G. de Marsily, and J. Andersson (1994). Solute Transport in Heterogeneous Media: A Discussion of Technical Issues Coupling Site Characterization and Predictive Assessment, *Advances in Water Resources*, Vol. 17, 259–264.

Tsang, C.F. and S.P. Neuman, editors (1992). *Report of the International INTRAVAL Project, Phase I*, Swedish Nuclear Power Inspectorate (SKI), Stockholm and OECD Nuclear Energy Agency, Paris.

Tsang, C.F., Y.W. Tsang, and F.V. Hale (1991). Tracer Transport in Fractures: Analysis of Field Data Based on a Variable-Aperture Channel Model, *Water Resour. Res.*, Vol. 27, No. 12, 3095–3106.

Tsang, Y.W. and C.F. Tsang (1987). Channel Model of Flow Through Fractured Media, *Water Resour. Res.*, 23, No. 3, 467–479.

Tsang, Y.W., and C.F. Tsang (1989). Flow Channeling in a Single Fracture as a Two-Dimensional Strongly Heterogeneous Permeable Medium, *Water Resour. Res.*, Vol. 25, No. 9, 2076–2080.

Tsang, Y.W. and C.F. Tsang (1993). Overview of Medium Heterogeneity and Transport Process. Invited Paper, Proceedings of International Workshop on Research and Development of Geological Disposal, Tokai, Japan, November 15–18, 1993. Power Reactor and Nuclear Fuel Development Corporation, Japan.

Tsang, Y.W., C.F. Tsang, F.V. Hale, and B. Dverstorp (1996). Tracer Transport in a Stochastic Continuum Model of Fractured Media, *Water Resources Research*, Vol. 32, No. 10, pp. 3077–3092.

Tsang, Y.W., C.F. Tsang, I. Neretnieks, and L. Moreno (1988). Flow and Tracer Transport in Fractured Media: A Variable Aperture Channel Model and Its Properties, *Water Resour. Res.*, 24, No. 12, 2049–2060.

Uchida, M., S. Sawada, T. Senba, M. Shimo, and T. Doe (1996). Hydrogeologic structure of granodiorite at the Kamaishi In-situ Experiment Site—A characterization of conductive fractures using pressure interference observation during borehole drilling. *Abstracts of 1996 Japan Earth and Planetary Science Joint Meeting*, Osaka, p. 670 (in Japanese with English abstract).

Williams, S.A., and A.I. El-Kadi (1986). COVAR–A Computer Program for Generating Two-Dimensional Fields of Autocorrelated Parameters by Matrix Decomposition, Int. Groundwater Modeling Cent., Holcomb Res. Inst., Butler Univ., Indianapolis, Ind.

Winberg, A., ed. (1996). First TRUE Stage—Tracer Retention Understanding Experiments, Descriptive structural-hydraulic models on block and detailed scales of the TRUE-1 site, by SKB TRUE Project Team, PNC/Golder Team, USDOE/LBNL Team. Swedish Nuclear Fuel and Waste Management Co., International Cooperation Report, 96-04.

Witherspoon, D.A., editor (1996). Geologic Problems in Radioactive Waste Isolation, Second Worldwide Review. Lawrence Berkeley National Laboratory Report LBNL-38915.

Table 1. Laboratory Experiments

Scale	Type of Experiments	References	Comments
5.2 cm	Injection of Wood's metal into fracture plane and observe its paths	Pyrak-Nolte et al. (1987)	Wood's metal flows to limited portion of the fracture plane
12 cm	Dyed water injected through core-center to fracture and emerging from rim of core	Gentier (1986) Gentier et al. (1989)	Emergency of dyed water very uneven at the rim of core traced by the fracture
19.5 cm	Traced water injected through a core with a fracture along its axis-breakthrough curves measured	Neretnieks et al., (1982) Moreno et al. (1985)	Tracer breakthrough curves cannot be described by advective-dispersive equation
41 cm	Flow through fracture along core axis; detailed measurements of apertures.	Hakami and Larsson (1996)	Irregular flow as a function of normal stress across fracture.

Table 2. Small Scale Field Experiments

2.5 m	Five boreholes in the plane of a fracture in granite; boreholes packed off in 7-cm section; crosshole pressure test	Bourke et al. (1987)	Found that only about 20% of fracture plane conducts water
1.95 m	Two boreholes in plane of a fracture; each hole packed off in 5 cm sections; crosshole tracer test. So-called "channeling experiment."	Abelin et al. (1988) Abelin et al. (1990)	Flow and transport highly channelized
5–10 m	Borehole into a fracture which is intercepted by a drift; flow and tracer emergence along the trace of fracture-drift intersection were studied. So called Stripa 2-D experiment.	Abelin et al. (1985)	Flow and transport highly uneven; fracture hydraulic aperture very different from fracture trace aperture.
20 m	A fracture shear zone intercepted by a drift and eight boreholes; flow and tracer transport measurements between boreholes in the fracture plane. So called MI experiment.	Frick et al. (1992) Eikenberg et al. (1994) Hadermann and Heer (1996)	Tracer breakthrough curves have fast rise, long tail, and multiple peaks in some cases. Patterns of flow very uneven in fracture plane-matrix diffusion detected.
10–20 m	Drift and boreholes intersect a 6-cm wide fracture zone. Drift wall is sectioned into collection areas	Birgersson et al. (1993)	Flow dominated by a few large flow paths. One out of 60 collection areas accounts for more than 50% of flow.
10.6–29.8 m	A single fracture. Dipole and radial converrgent flow field and pulse tracer injection.	Novakowski et al. (1985); Raven et al. (1988)	Able to fit the data with a "transient solute storage model" with mobile and stagnant flow zones in the fracture.

Table 3. Large Scale Field Experiments

Scale	Type of Experiments	References	Comments
25–75 m	Drift of 100 m and 3 boreholes from drift into fractured rock; tracers injected through packed intervals in boreholes. Flow and tracers observed in collection sheets on drift walls. So called Stripa 3-D experiment.	Neretnieks (1987) Abelin et al. (1987)	Flow and tracer breakthroughs very uneven. Tracer breakthrough curves cannot be described by advective dispersive equation.
25–100 m	Drift of 100 m with radial boreholes into highly fractured rocks. Injection flows measured in packed intervals in boreholes; tracer injected into intervals and collected in sections of drift. So called Faray Augers experiment.	Calmels et al. (1986) Barbreau et al. (1987)	Data used to calibrate models by stochastic methods (matching distribution).
150–200 m	Injection and withdrawal wells drilled into a fracture zone 100–260 m below ground. Flow and tracer experiments were made. The latter include both single well convergent and dipole-well interflow experiment. So called Finnsjön experiment.	Andersson et al. (1988; 1989) Andersson et al. (1990)	Multiple tracers used. Many tracer breakthrough curves, all with long tails and some with multiple peaks.
50–150 m	Shafts and boreholes into three fracture zones; tracers injected through packed intervals in boreholes and collected at shafts (URL, Whiteshell, Canada).	Frost et al. (1992) Frost and Davison (1994)	Tracer breakthrough curves vary from those describable by advective dispersive equation to those with long tails and multiple peaks.
1000 m	A tunnel and silo system in fractured rock under Baltic, at Forsmark observes inflows on tunnel wells.	Neretnieks (1994)	Inflows very spotty on rock walls; strong variability in flow rates.

Other On-Going Experiments

- Kamaishi Mines – PNC, Japan (Sawada et al., 1996; Uchida et al., 1996)
- HRL, Aspo – SKB, Sweden (Bäckblom, 1995; Winberg, 1996)
- WIPP/Culebra – SNL, USA (Jones et al., 1992; Beauheim et al., 1995)

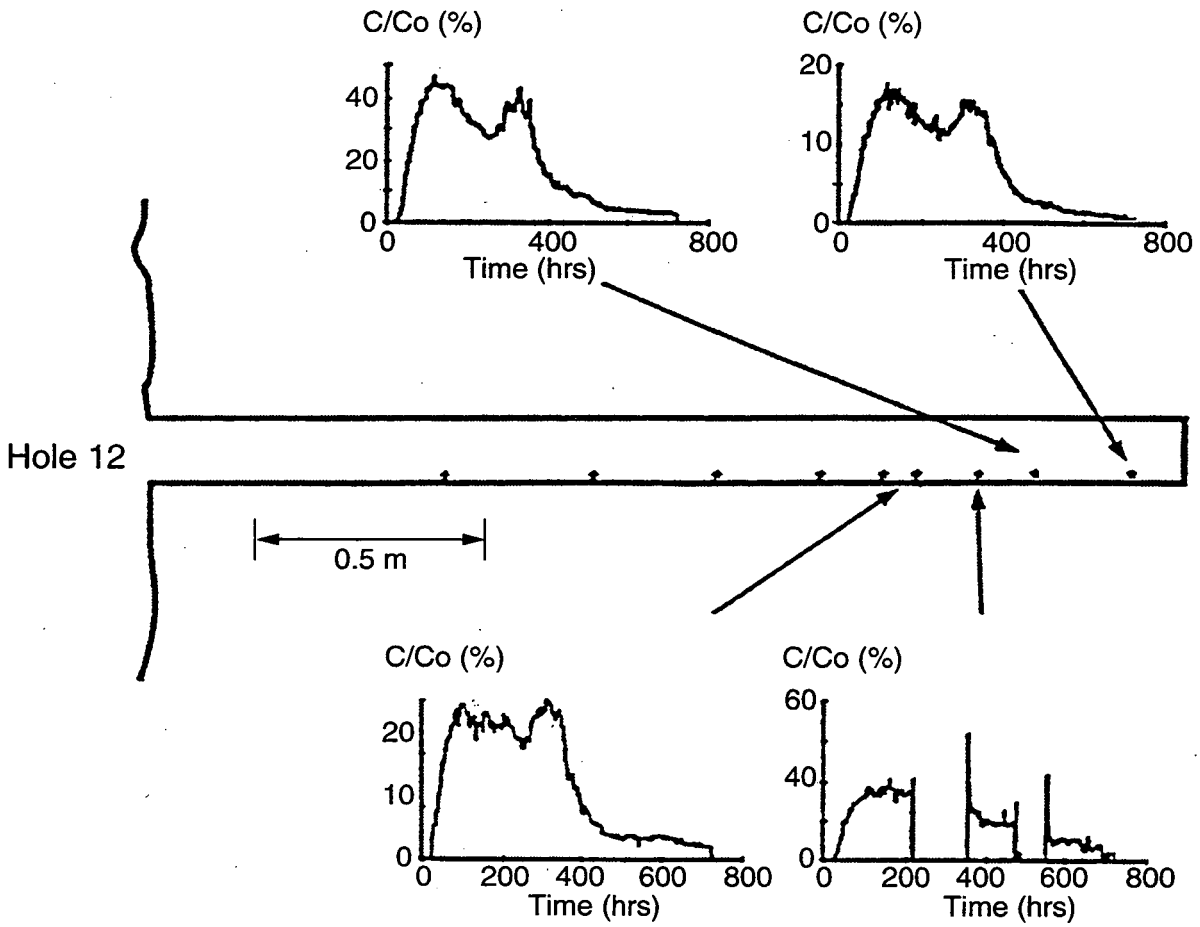

Figure 6. Tracer breakthrough curves at various points in the pumping Hole 12 (see Figure 5). (Taken from Abelin et al., 1990.) The lower right curve shows two intervals of no data due to experimental difficulties.

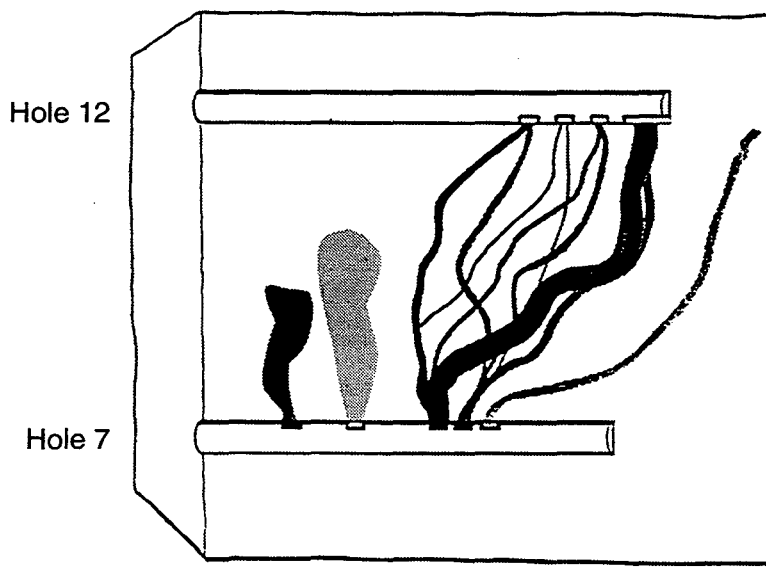

Figure 5. Diagram of flow of tracers from one borehole (Hole 7) to the other (Hole 12) in the same fracture plane based on data of responses between packed intervals of the boreholes. The two holes are separated by 1.95 meters. (Taken from Abelin et al., 1990.)

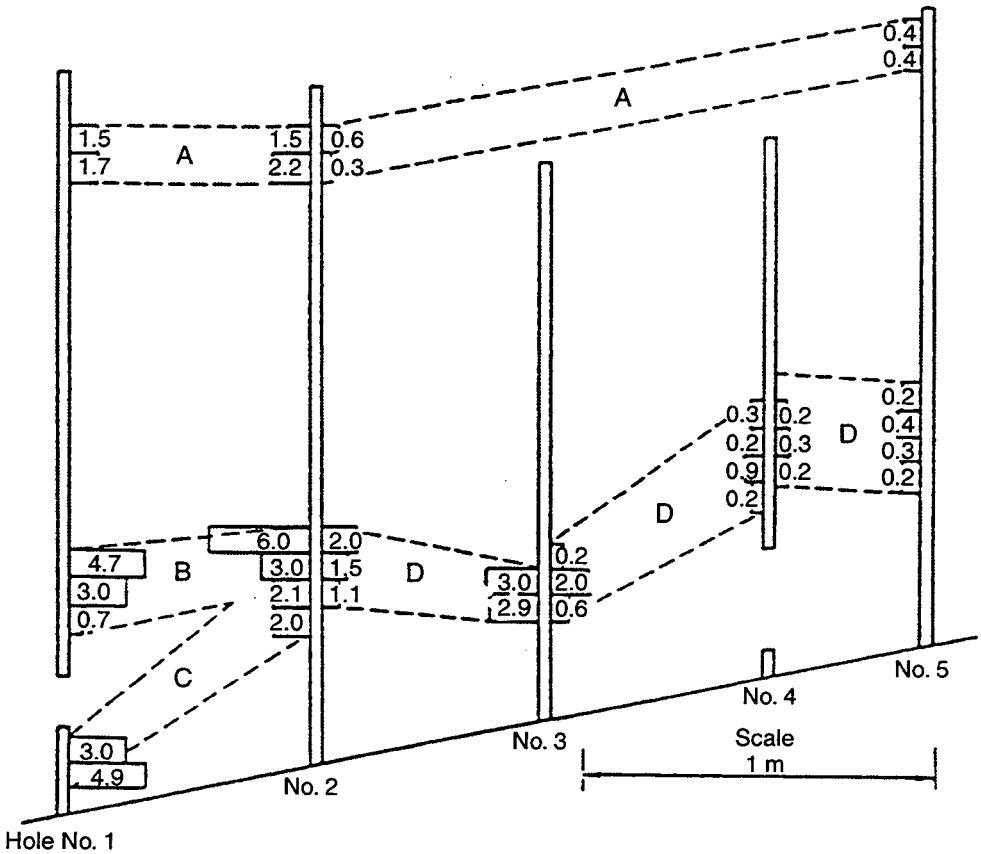

Numbers on histograms are flows in ml/sec from adjacent holes

Figure 4. Flow channeling in the plane of a single fracture. The five boreholes are drilled in the fracture plane, which is, however, not entirely flat; thus some parts of boreholes are outside the fracture plane. Flow channels are indicated as A, B, C and D. (Taken from Bourke, 1987.)

(a)

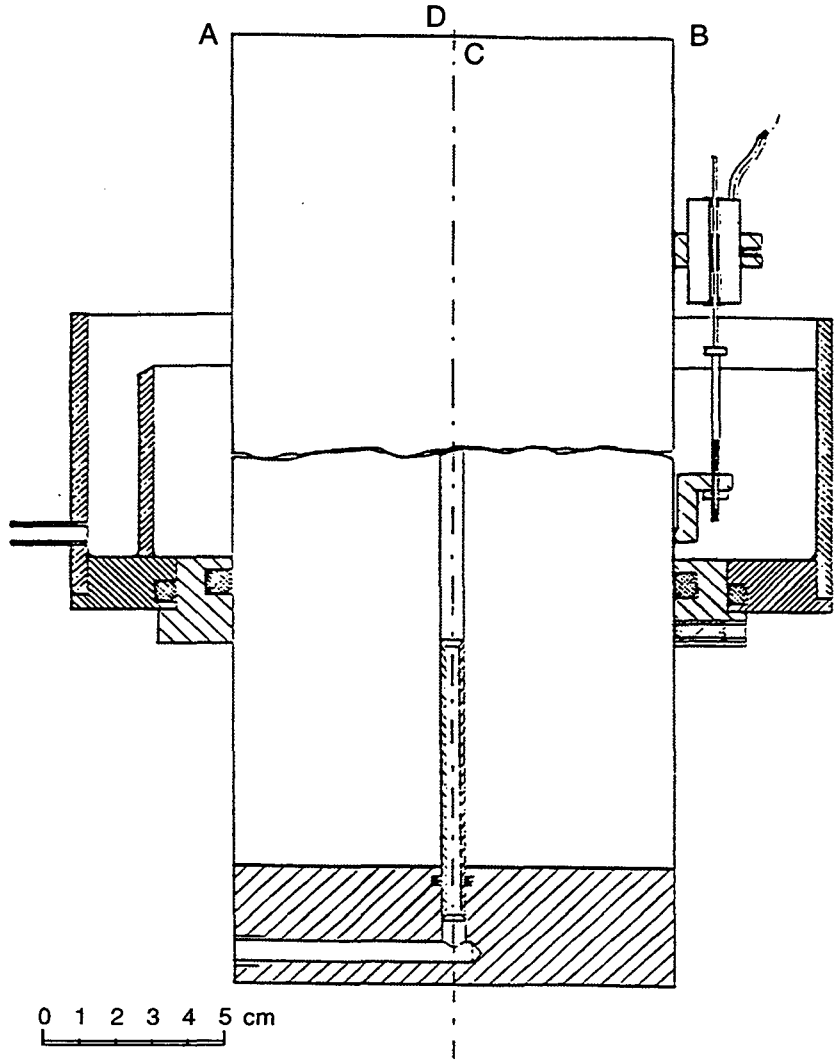

(b)

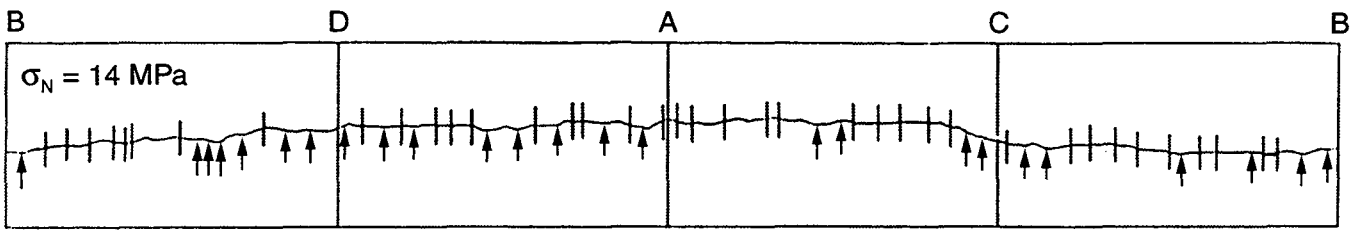

Figure 3. (a) Laboratory set up by Gentier et al. (1989) to study radial flow in a fracture across a core sample. (b) Outflow points (vertical arrows) along the circumferences of a single fracture in a core sample. (Taken from Gentier, 1986.)

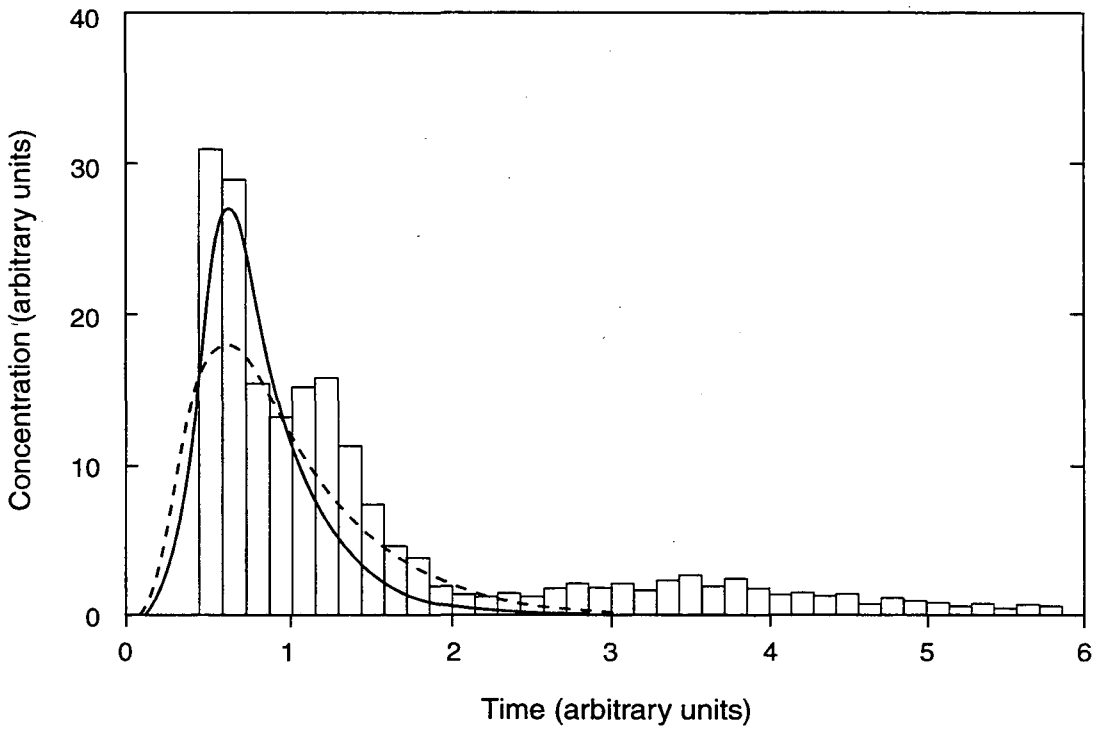

Figure 2. Tracer breakthrough curve: the histogram is the result based on calcuated flow in a variable-aperture fracture; and the two curves (solid and broken lines) are solutions (Equation 10) of the advective-dispersive equation with two sets of D, v values.

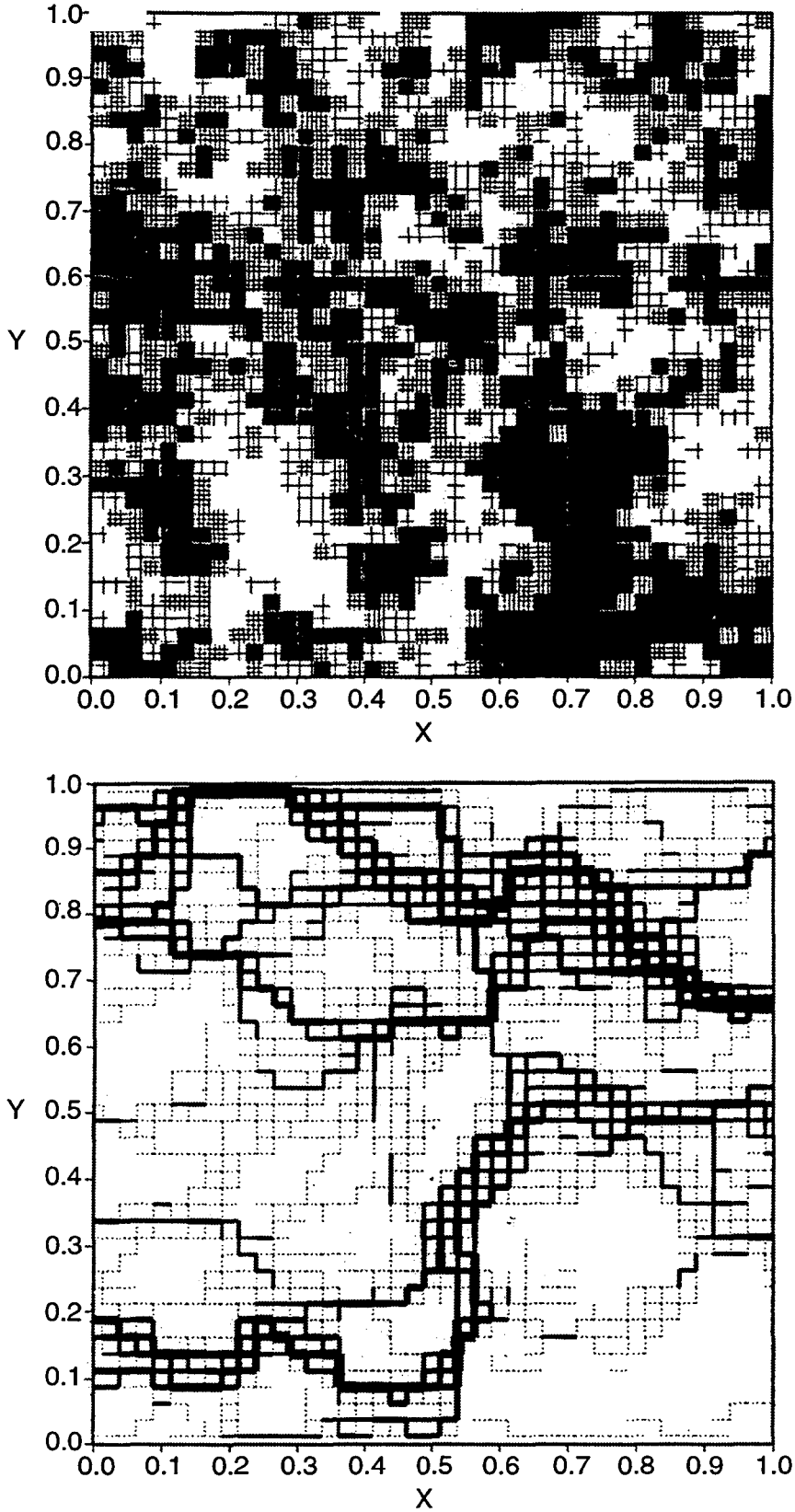

Figure 1. Schematic calculation to illustrate flow channeling. Top figure shows permeability variations, with darker areas having lower permeability values. Lower figure shows flow rates under imposed pressure gradient from left to right, the thickness of lines being proportional to square root of flow rates. (Taken from Moreno et al., 1990.)

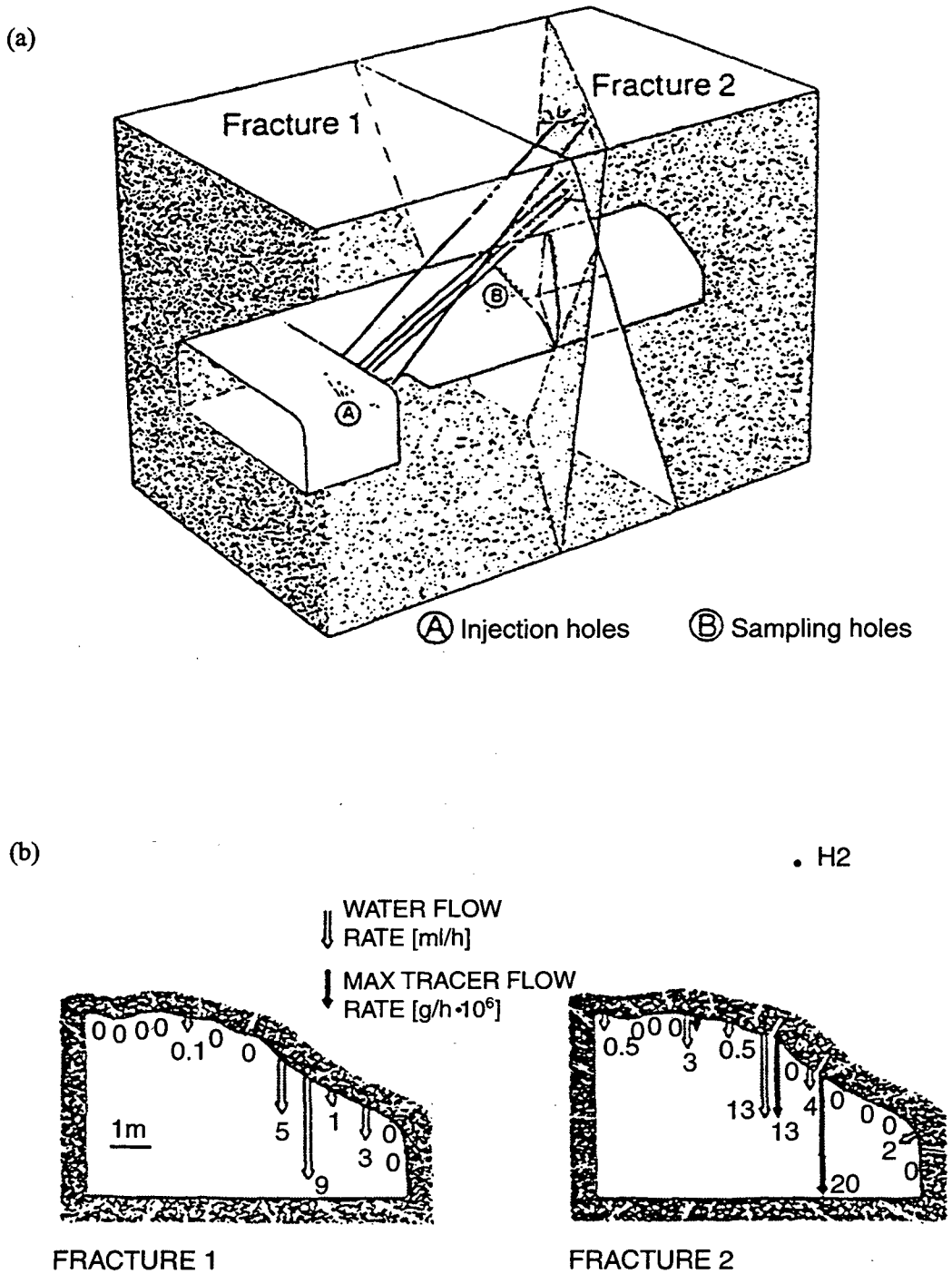

Figure 7. (a) Experimental set up of Stripa 2D Experiment. (b) Water and tracer emergence points along fracture traces in Stripa 2D experiment, illustrating strong channelization. (Taken from Abelin et al., 1985.)

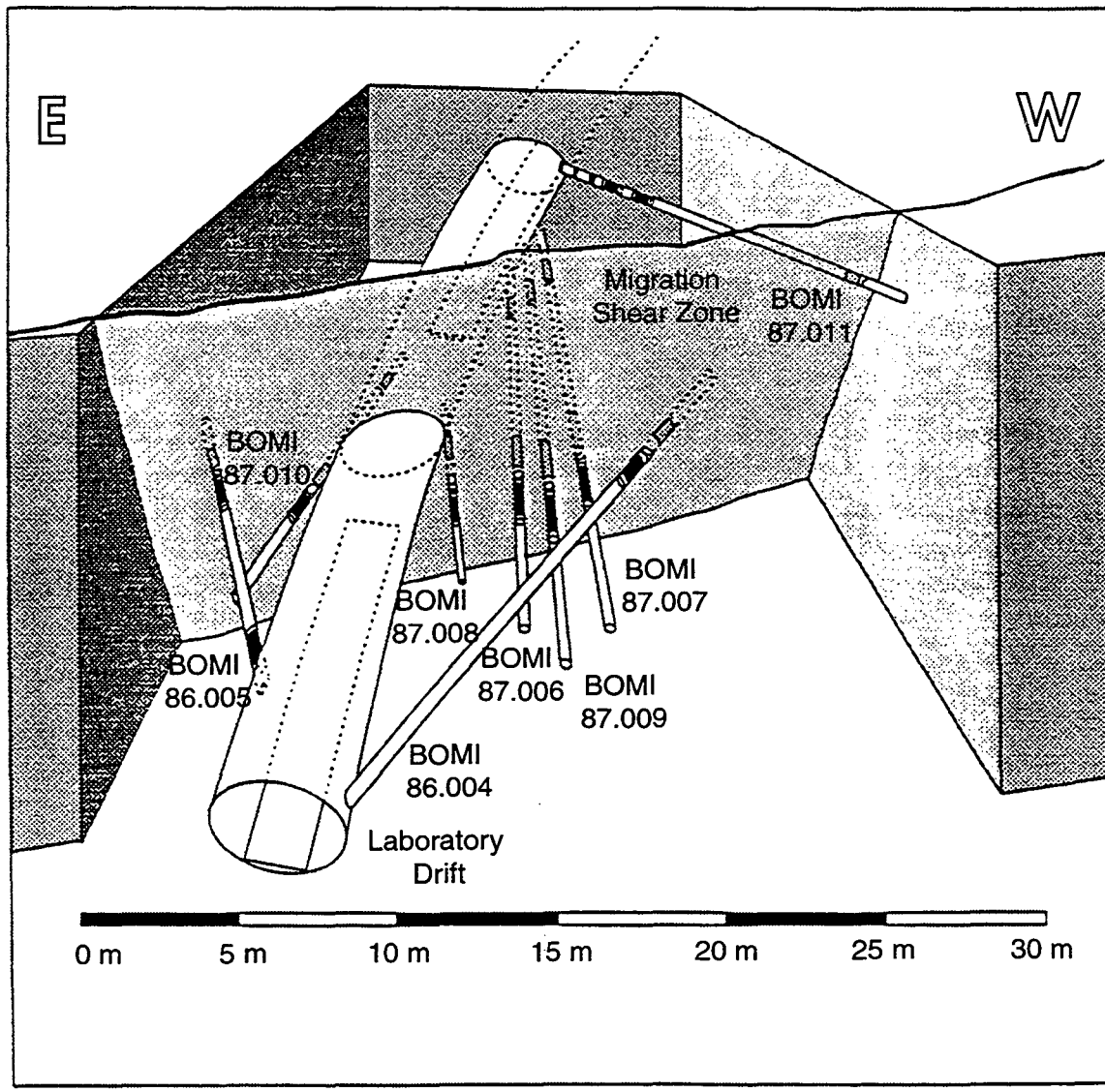

Figure 8. Experimental set up of the MI experiment in Grimsel Test site in Switzerland. The boreholes are packered off at the fracture zone labelled "Migration Shear Zone." (Taken from Eikenberg et al., 1995.)

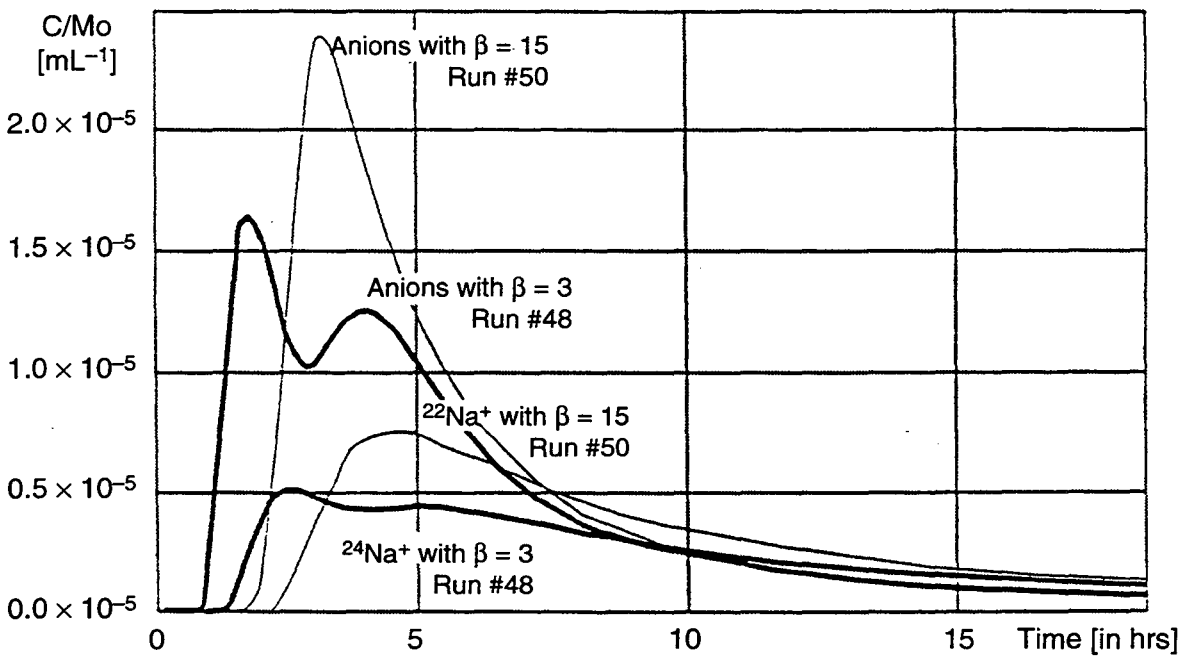

Figure 9. An example sample of tracer breakthrough curves obtained in the Grimsel MI experiment, illustrating the sharp rise, long tail, and multiple peaks features. (Taken from Eikenberg et al., 1994.)

(a)

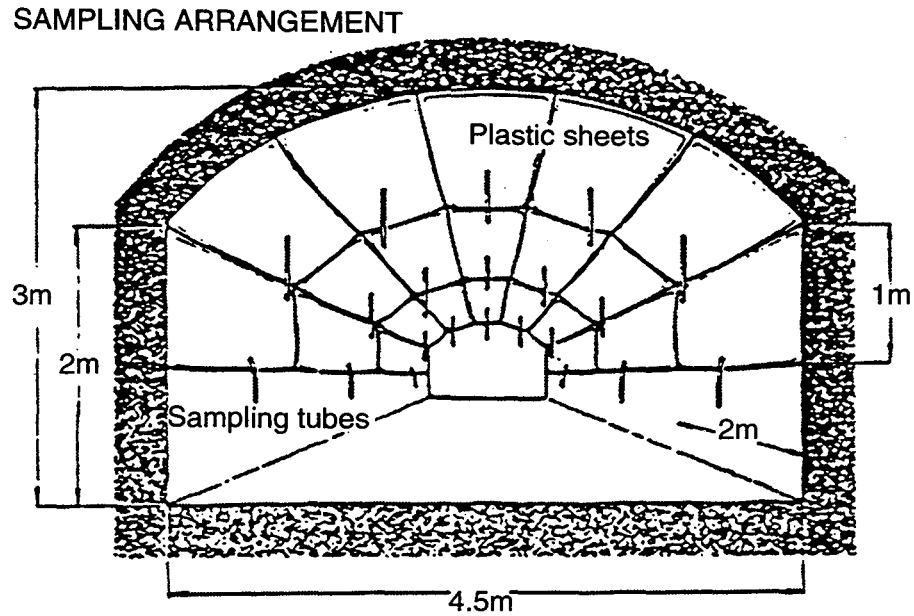

(b)

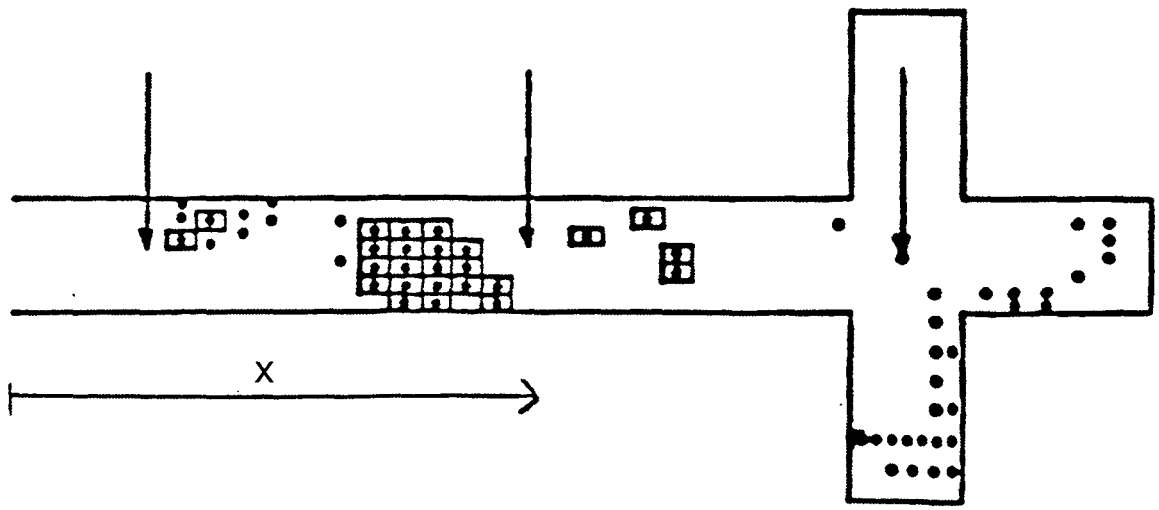

Figure 10. (a) Experiment set up for collecting tracer flow in the drift in the Stripa 3D experiment. (b) Observations of emergence of flow (dots) and tracers (rectangles) in the drift. (Taken from Abelin et al., 1987.)

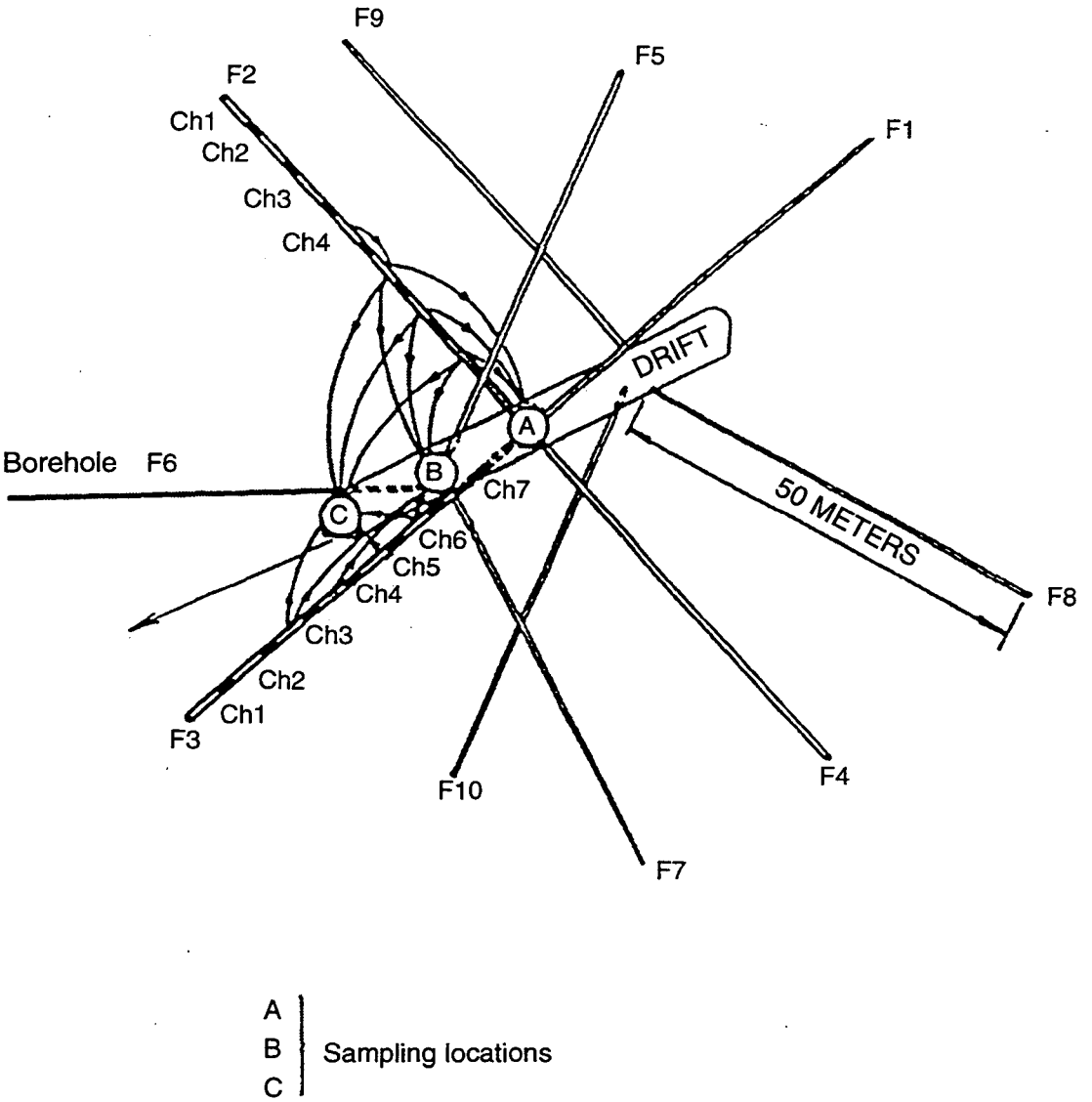

Figure 11. Experiment set up of the Fanay-Augeres Experiment. (Taken from Cacas et al., 1990.)

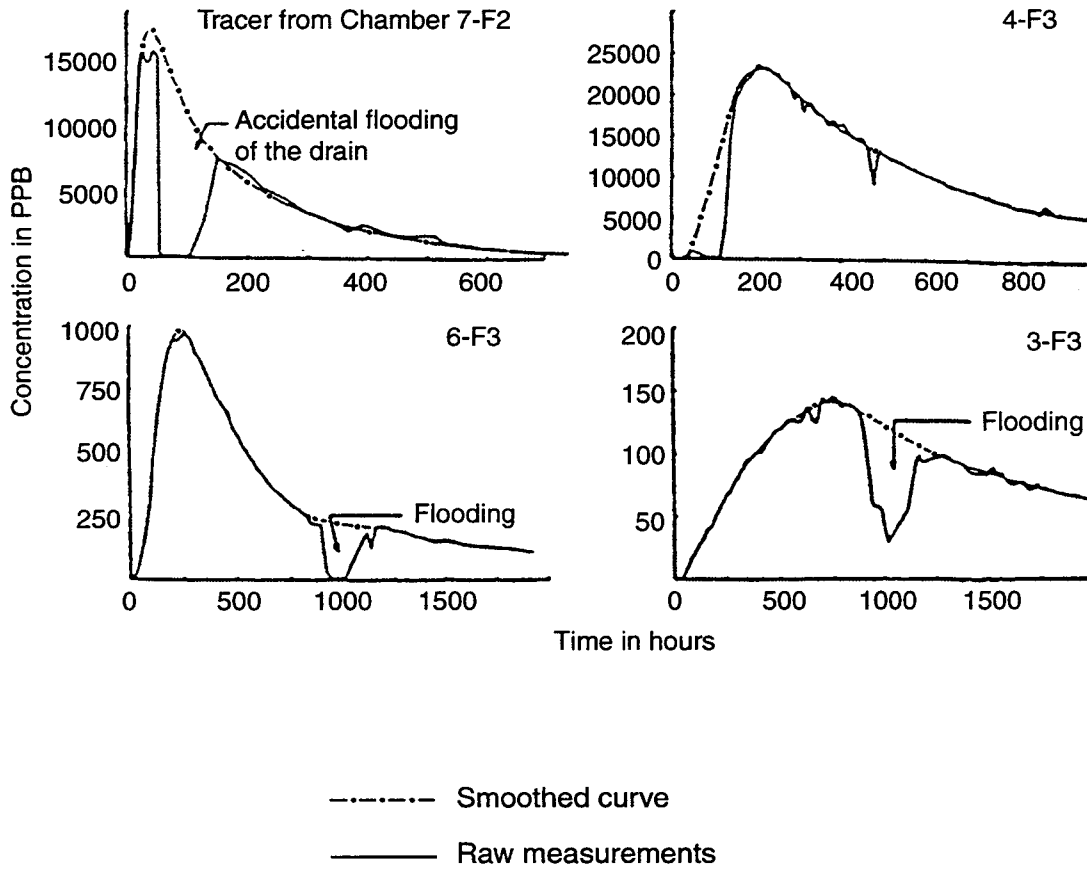

Figure 12. Examples of tracer breakthrough curves obtained in the drift with tracer injection in boreholes in the fracture rock around the drift at Fanay Augeres. (Taken from Cacas et al., 1990.)

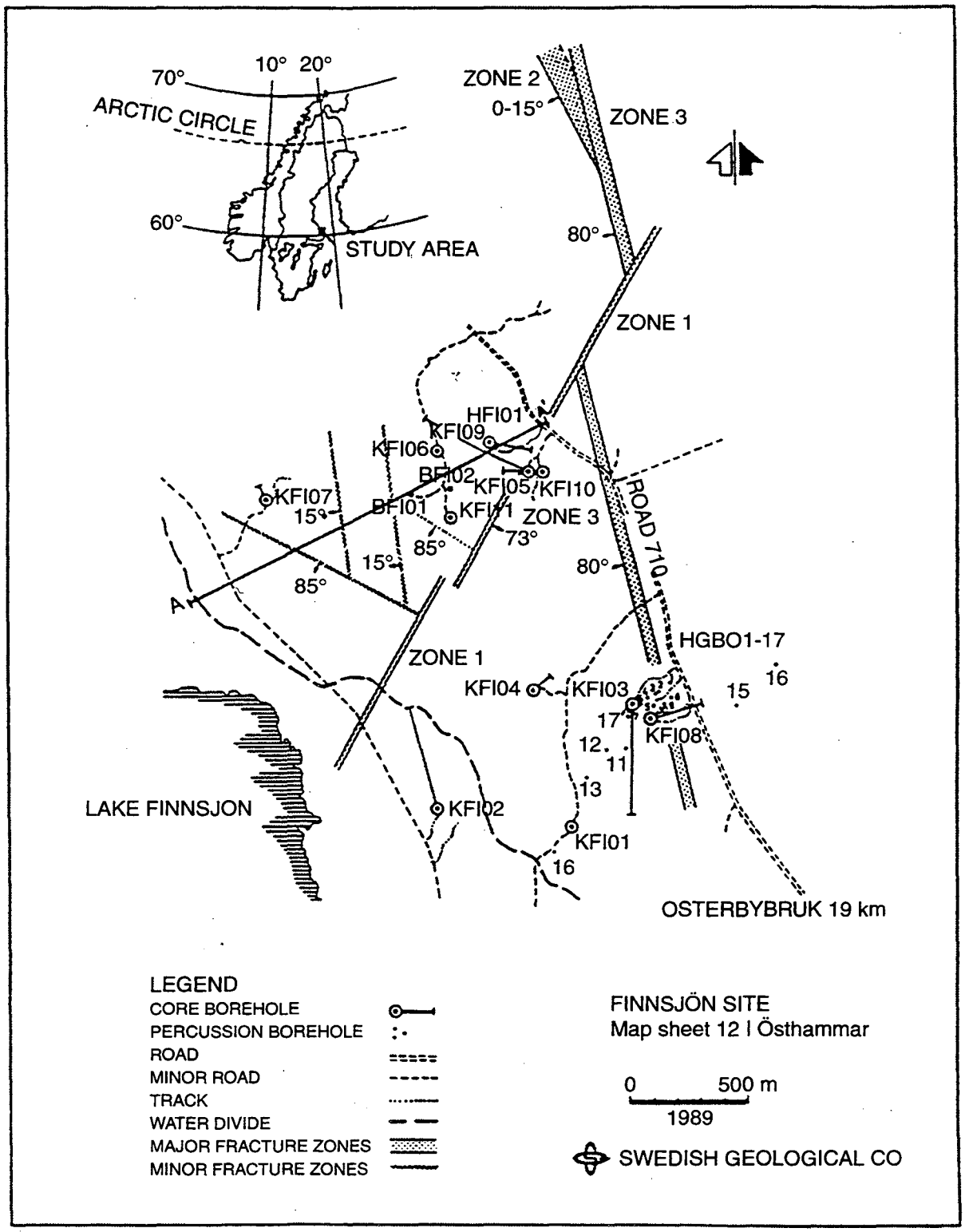

Figure 13. Map showing the site of the Finnsjon Experiment performed by Andersson and coworkers of the Swedish Geological Company. (Taken from Andersson et al., 1989.)

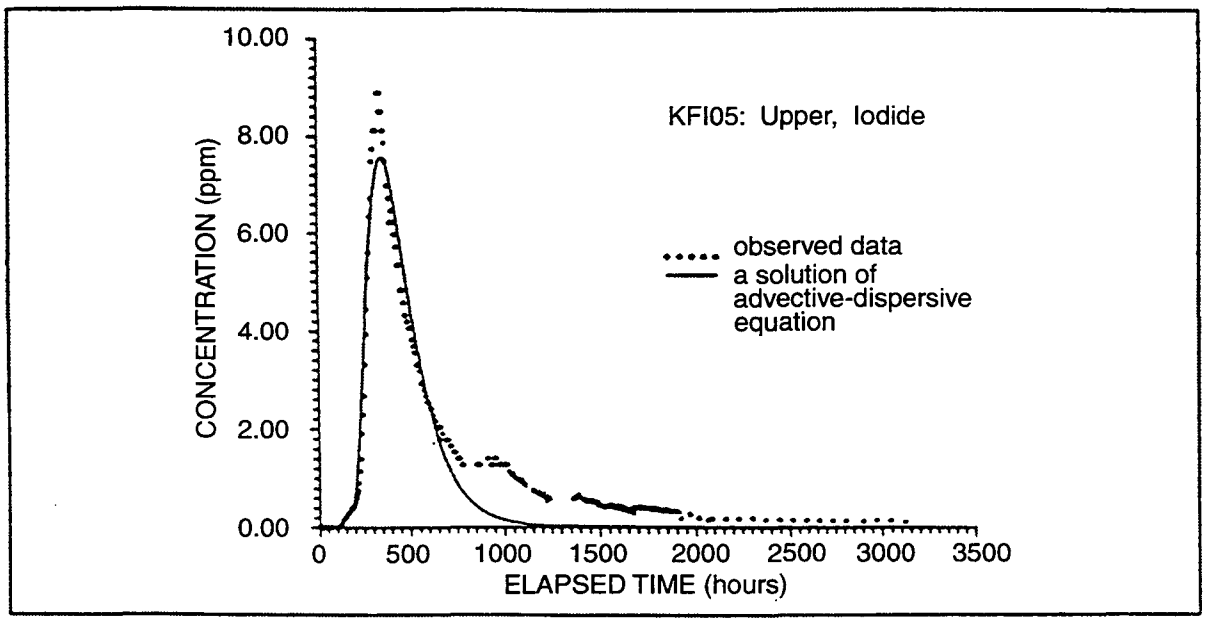

Figure 14. An example of the tracer breakthrough curves obtained in the Finnsjon Experiment. (Taken from Tsang and Neuman, 1992.)

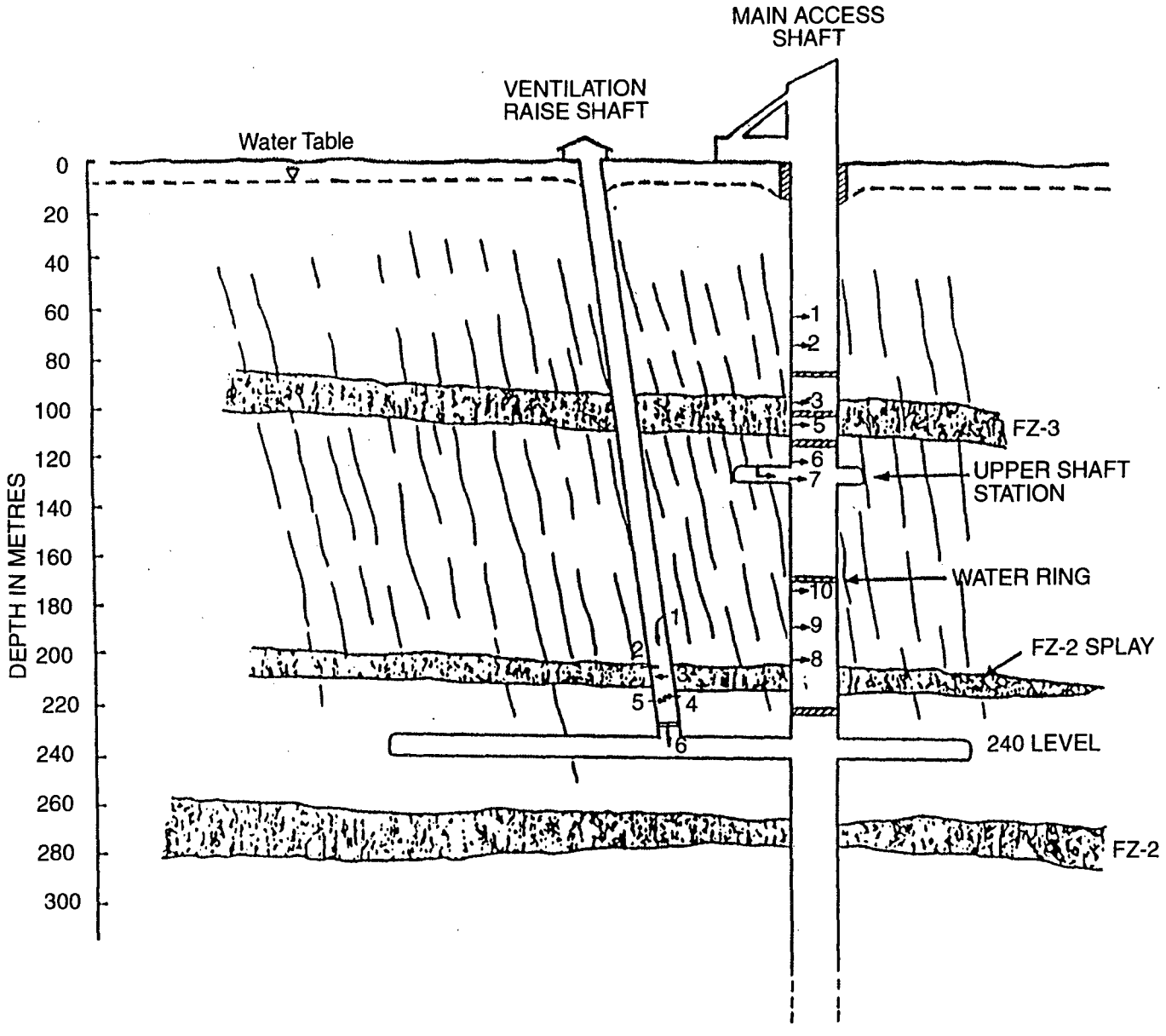

Figure 15. Schematic diagram of vertical cross section of the Underground Research Laboratory at Whiteshell, Canada. Fracture zones are labelled FZ-3, FZ-2 and FZ-2 SPLAY. (Taken from Frost and Davison, 1994.)

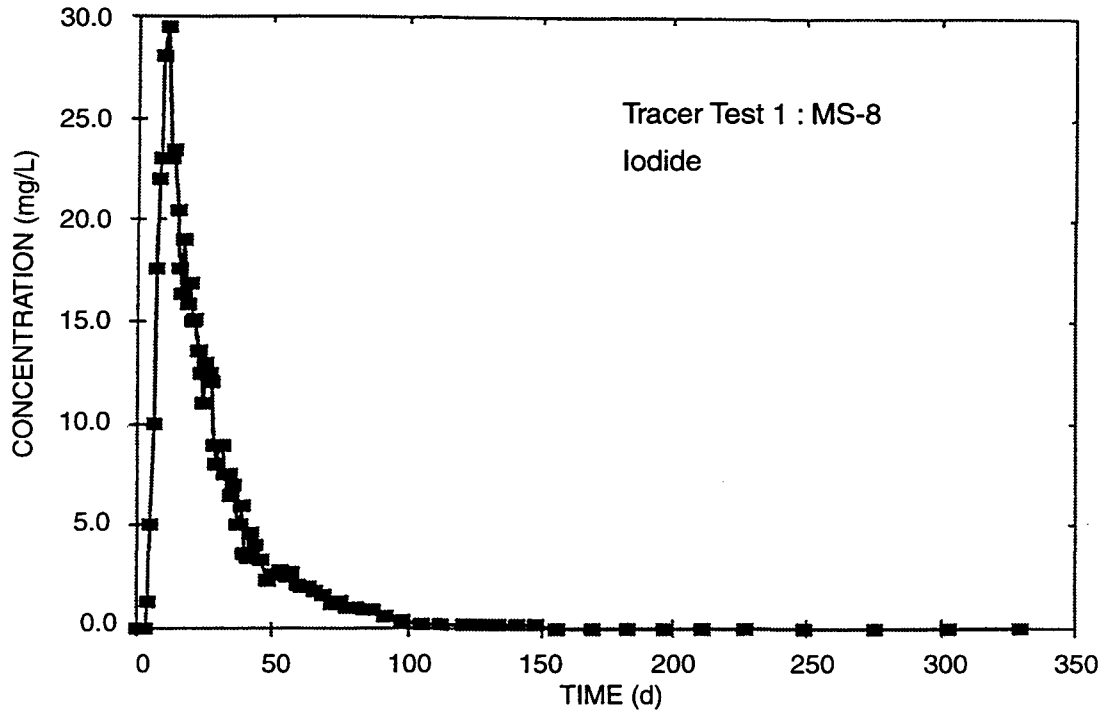

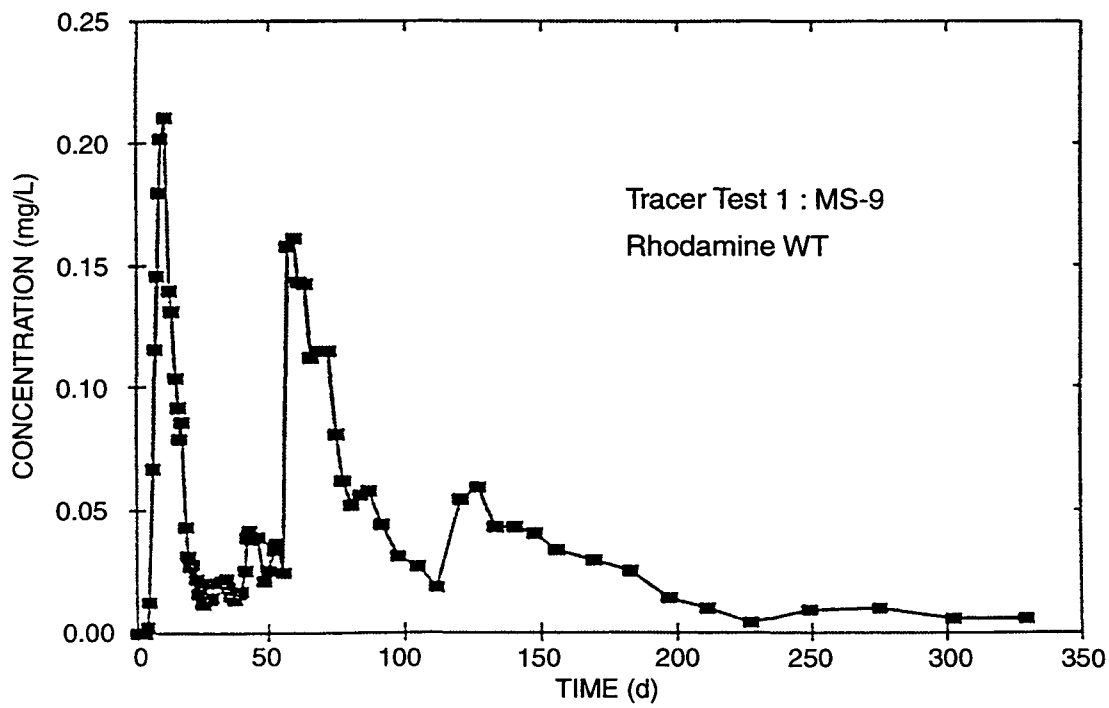

Figure 16. Typical tracer breakthrough curves from experiments of tracers injected in FZ3 and observed in the section 8 and 9 of the main shaft (MS-8 and MS-9 respectively) at URL, Canada. (Taken from Frost and Davison, 1994.)

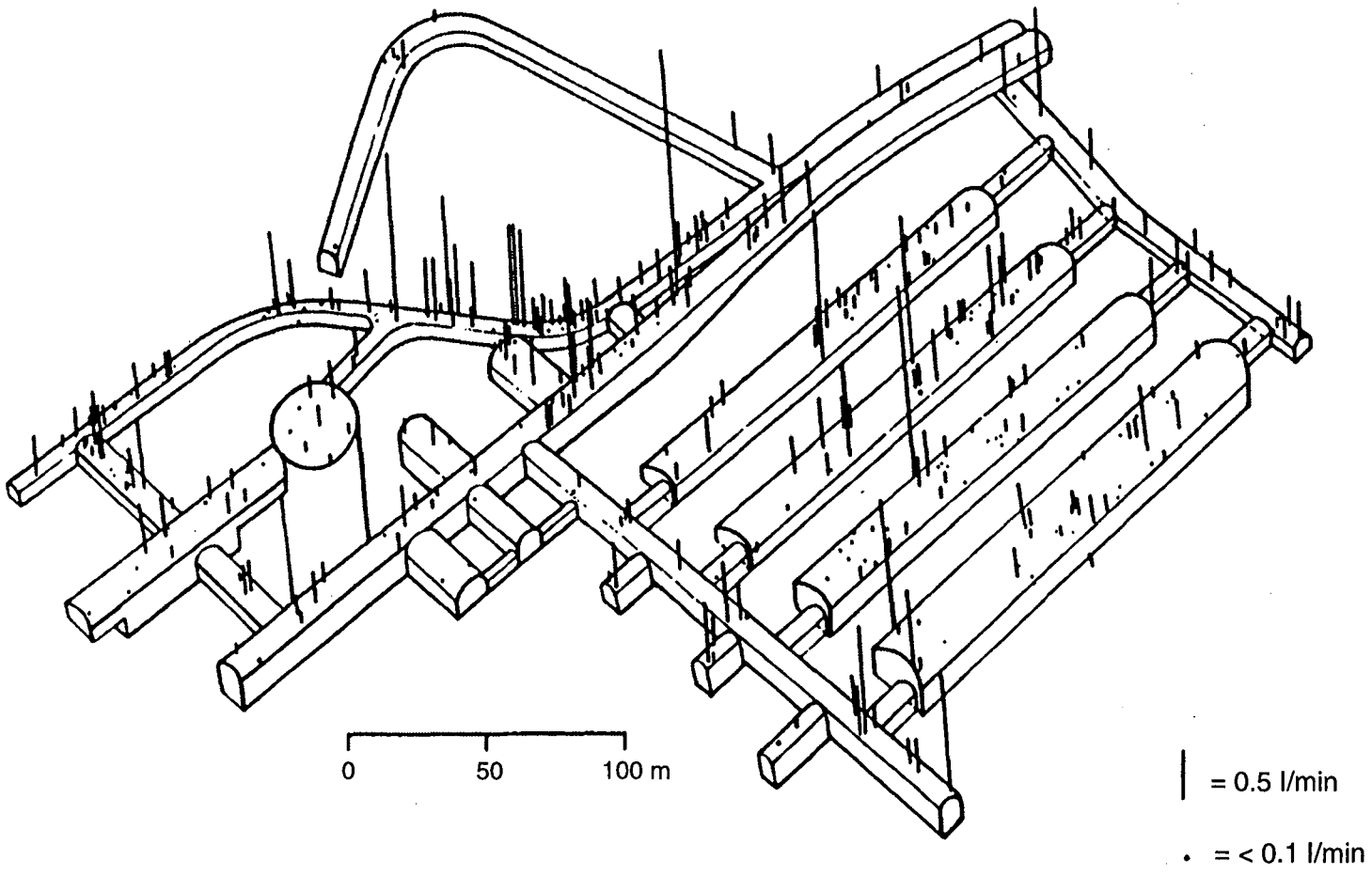

Figure 17. Overview of the drifts at the SFR site, Forsmark, Sweden. The length of the bars is proportional to the flowrates observed in the drifts.

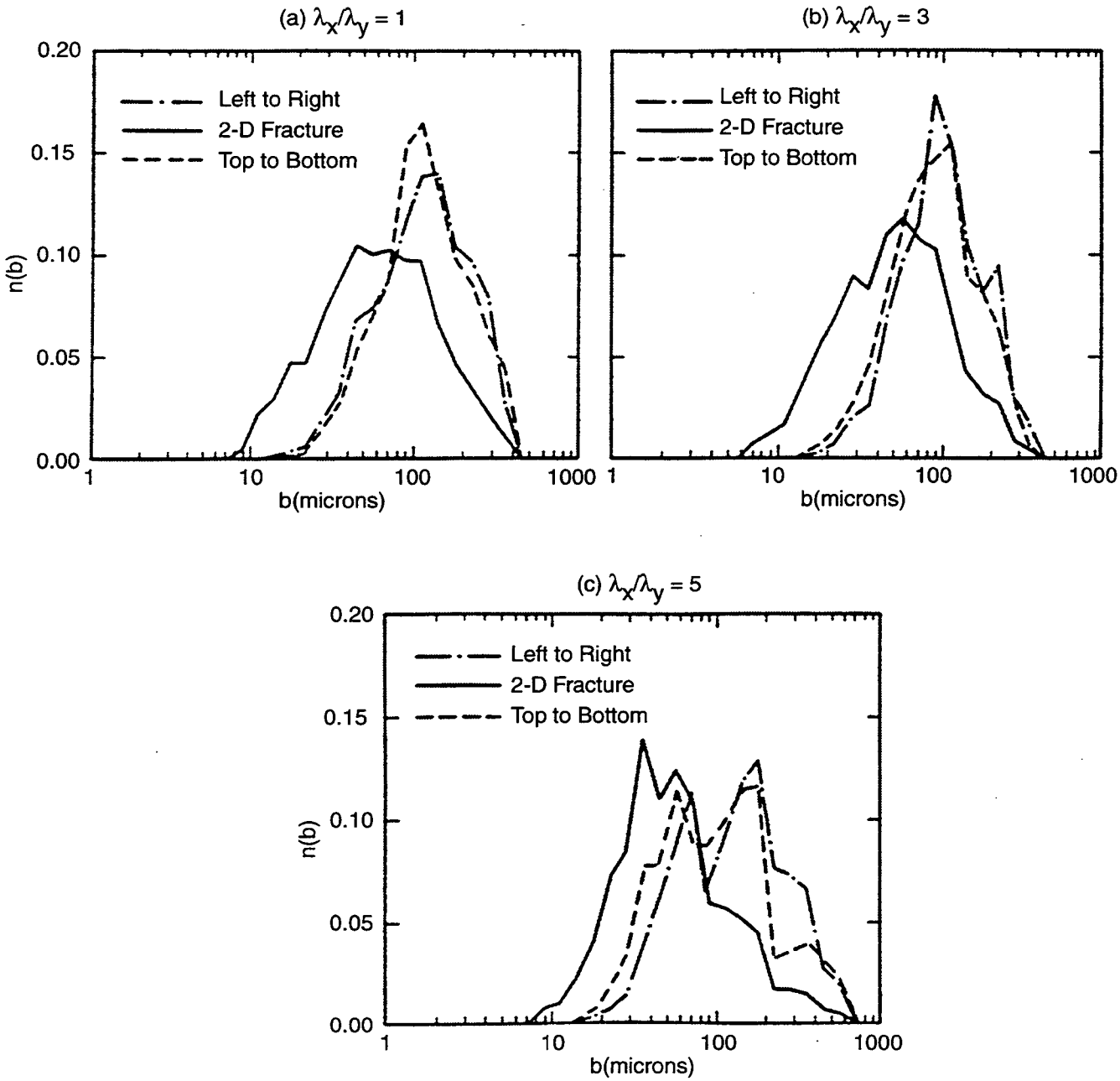

Figure 18. The probability distribution n(b) of fracture aperture values b over the fracture surface (solid lines), along flow paths under left-right pressure difference (dot-dash lines), and along flow paths under top-bottom pressure difference (broken lines), for three realizations of single fractures with different anisotropies (λ_x/λ_y). (From Tsang and Tsang, 1989.)

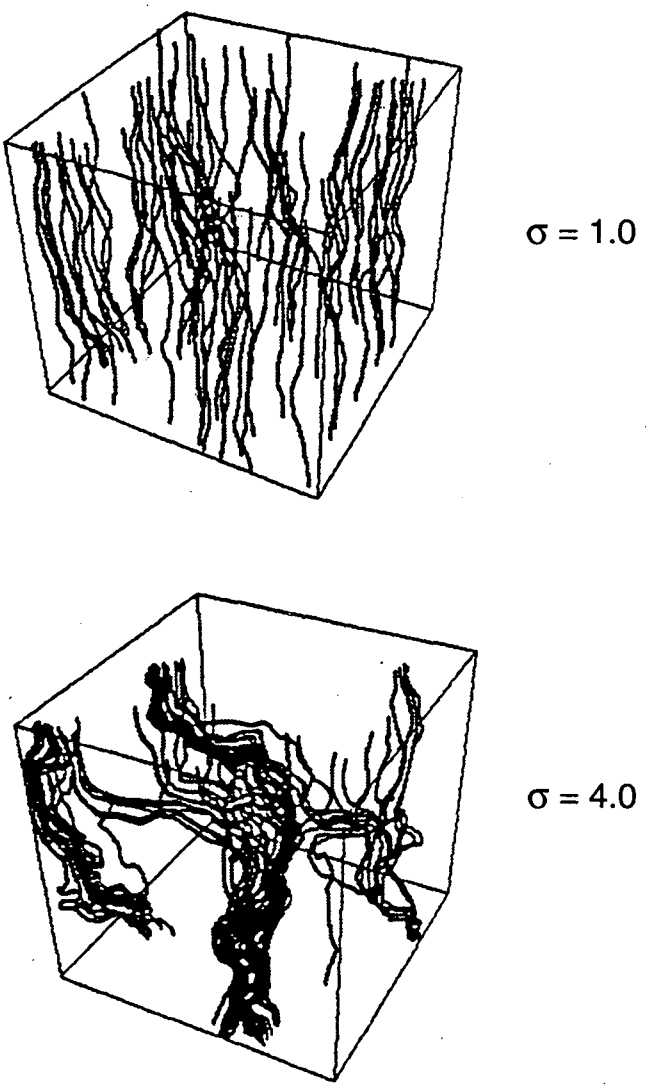

Figure 19. Flow lines of solutes through a heterogeneous medium under pressure difference from top to bottom for two degrees of heterogeneity given by the standard deviations in natural log permeability values. (Taken from Moreno and Tsang, 1994.)

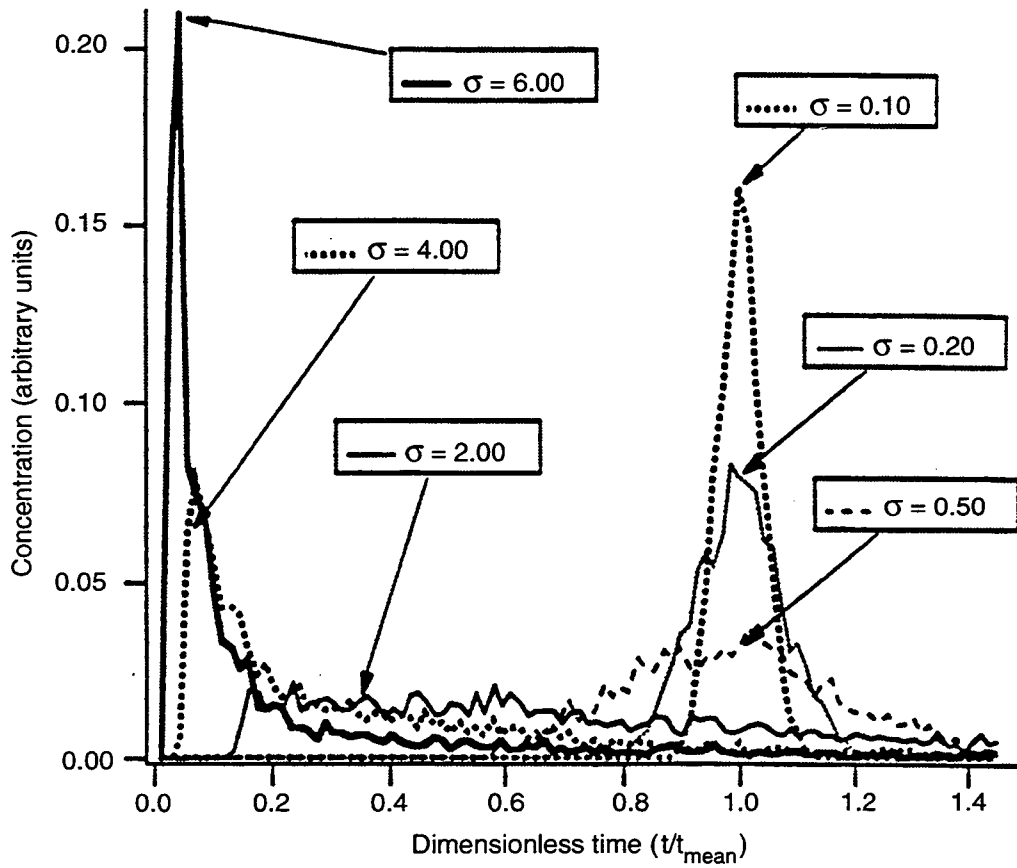

Figure 20. Tracer breakthrough curves for flow through a heterogeneous porous medium block for different values of standard deviation σ in natural log. Time is normalized to the mean arrival time. (Taken from Moreno and Tsang, 1994.)

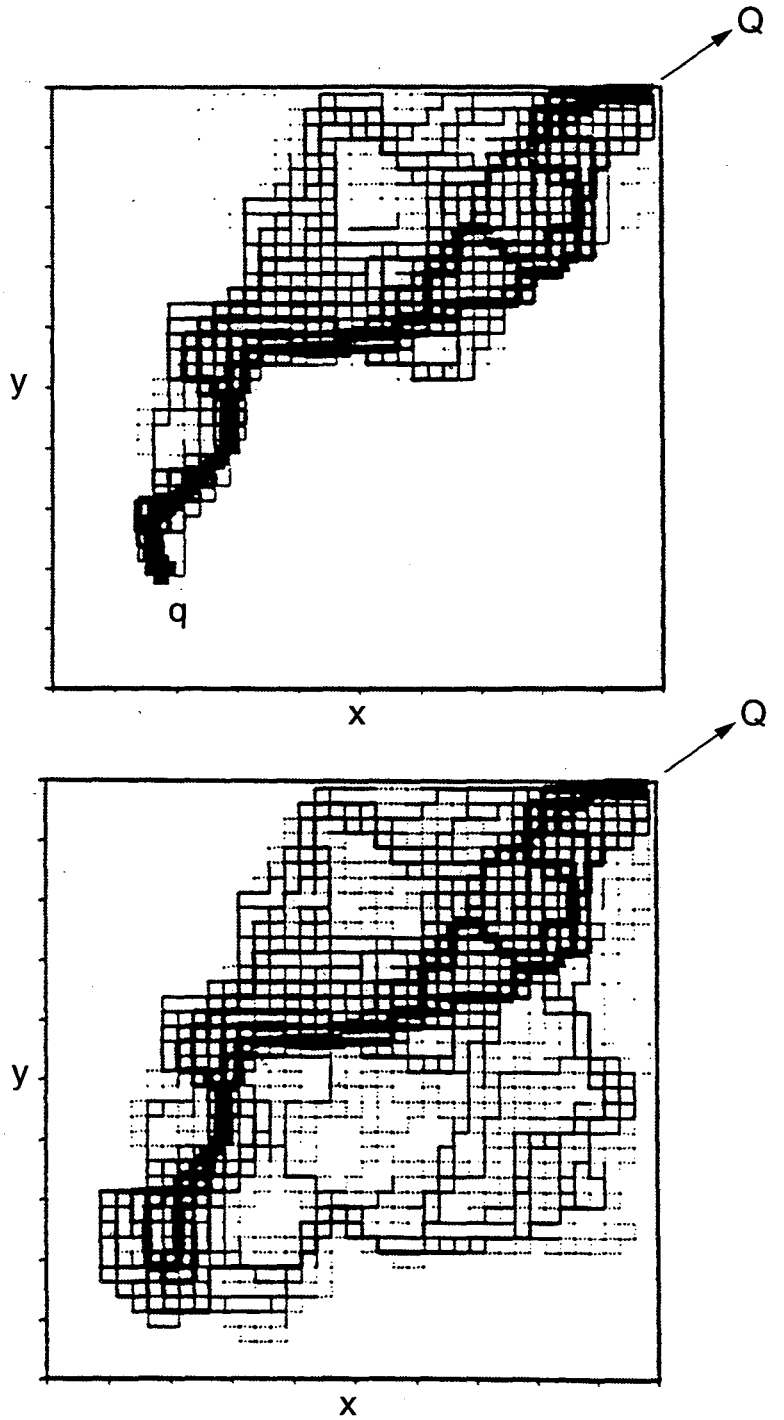

Figure 21. Tracer flow paths to a pumping well with flow rate Q at the upper right corner, from an injection point from a point in the lower left part of the flow region. The top figure shows the case of tracer injection rate q at 0.003 Q, and the lower figure, the case of q = 0.03 Q. (Taken from Moreno and Tsang, 1991.)

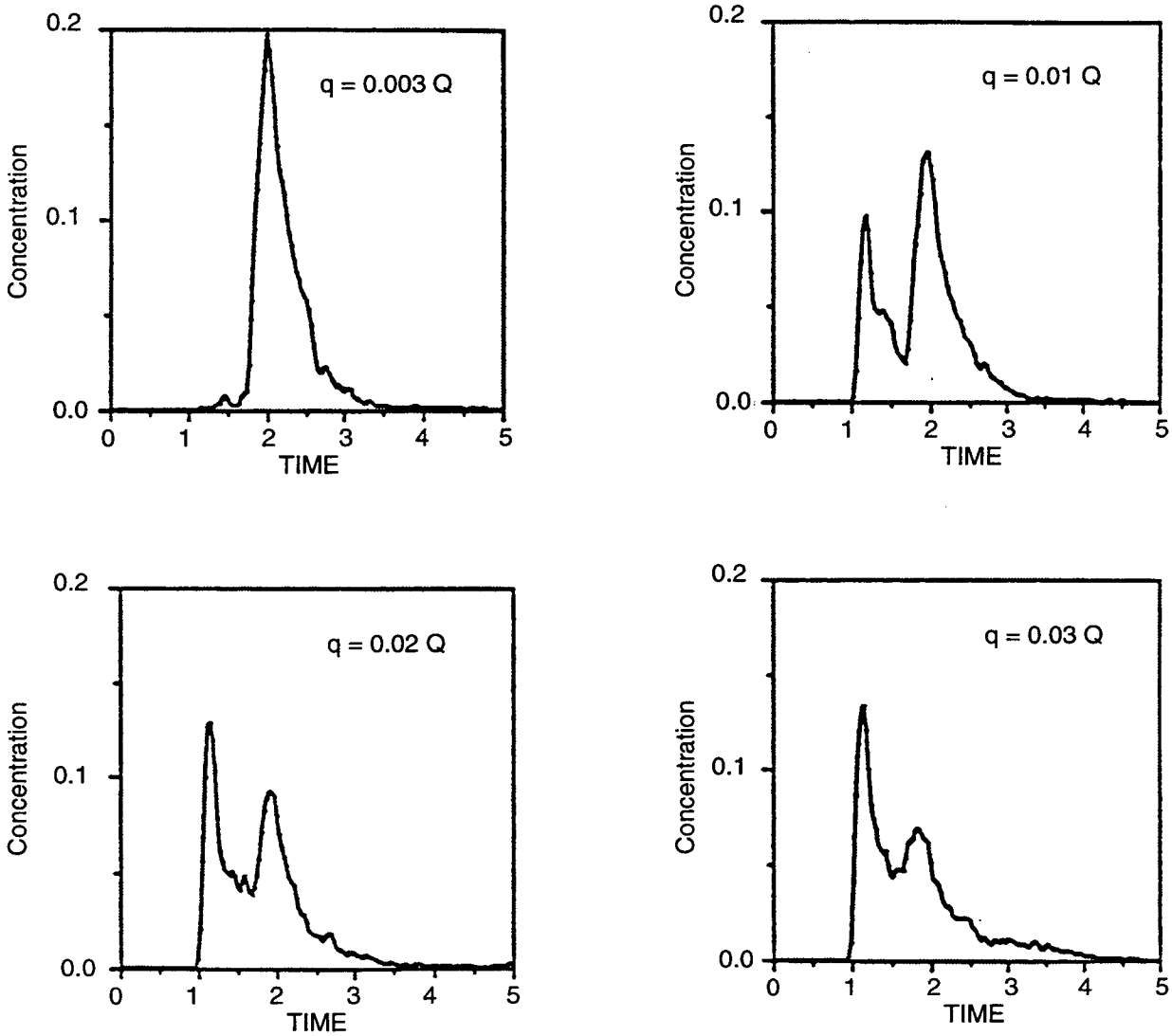

Figure 22. Tracer breakthrough curves corresponding to Figure 21, with q = 0.003 Q, 0.001 Q, and 0.02 Q and 0.03 Q. (Taken from Moreno and Tsang, 1991.)

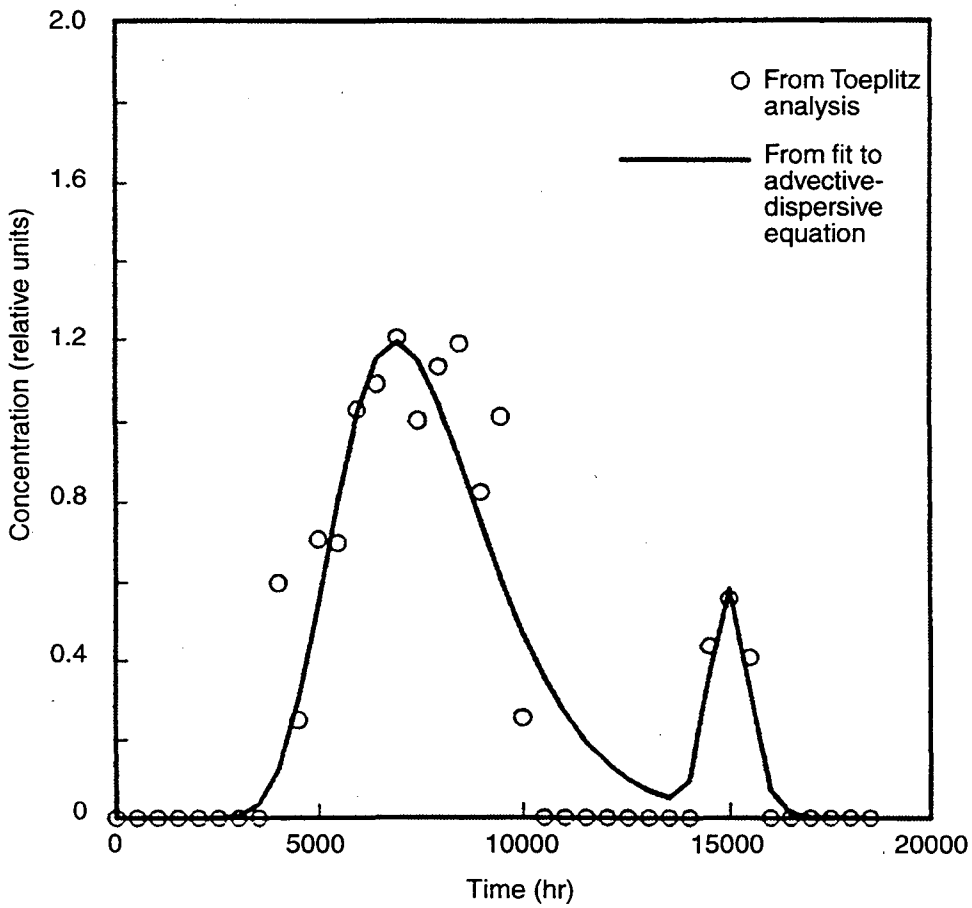

Figure 24. Results of Toeplitz analysis method for Iodide, to show equivalent breakthrough curve for a pulse tracer test. The two peaks are fitted by two solutions of the linear advective-dispersive equation.

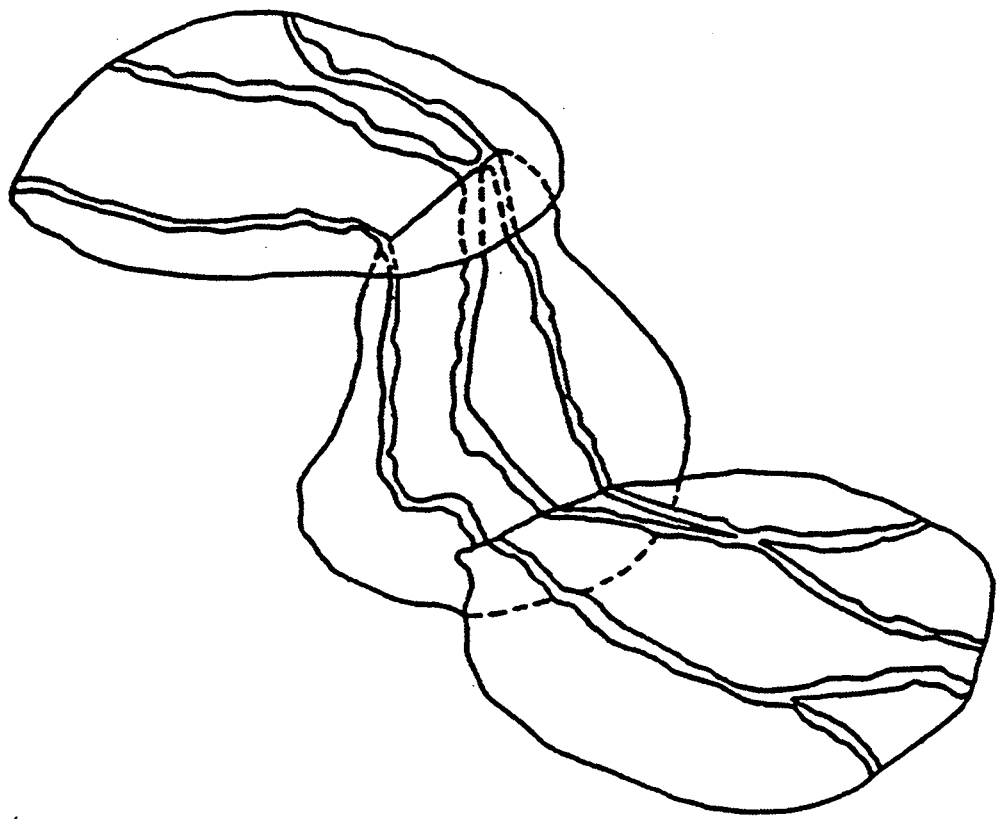

Figure 23. Conceptual picture of flow channeling through three intersecting fractures. (Taken from Tsang et al., 1991.)

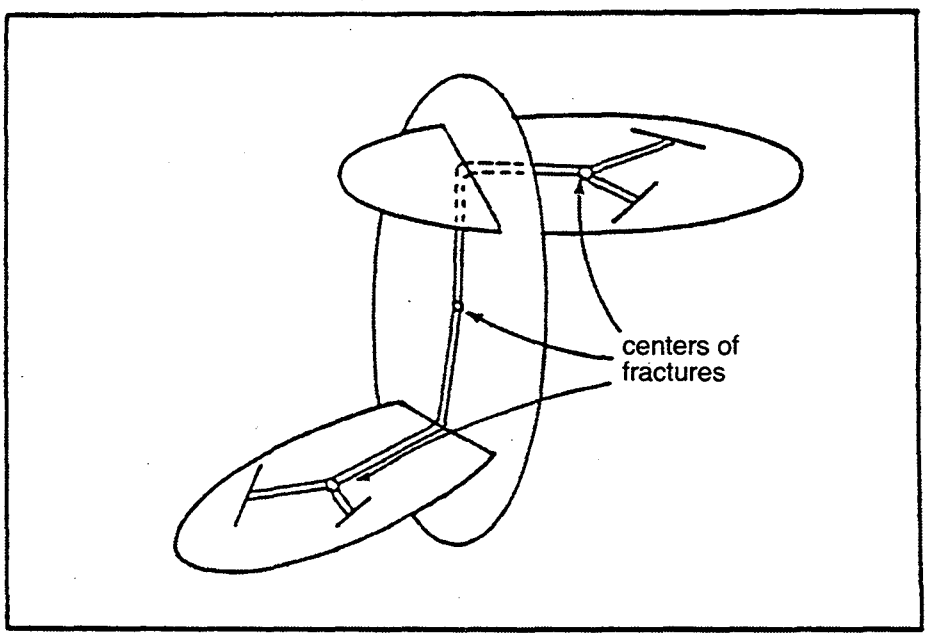

Figure 25. Conceptual model of a channel network to represent a multiple fracture system. (Taken from Cacas et al., 1990.)

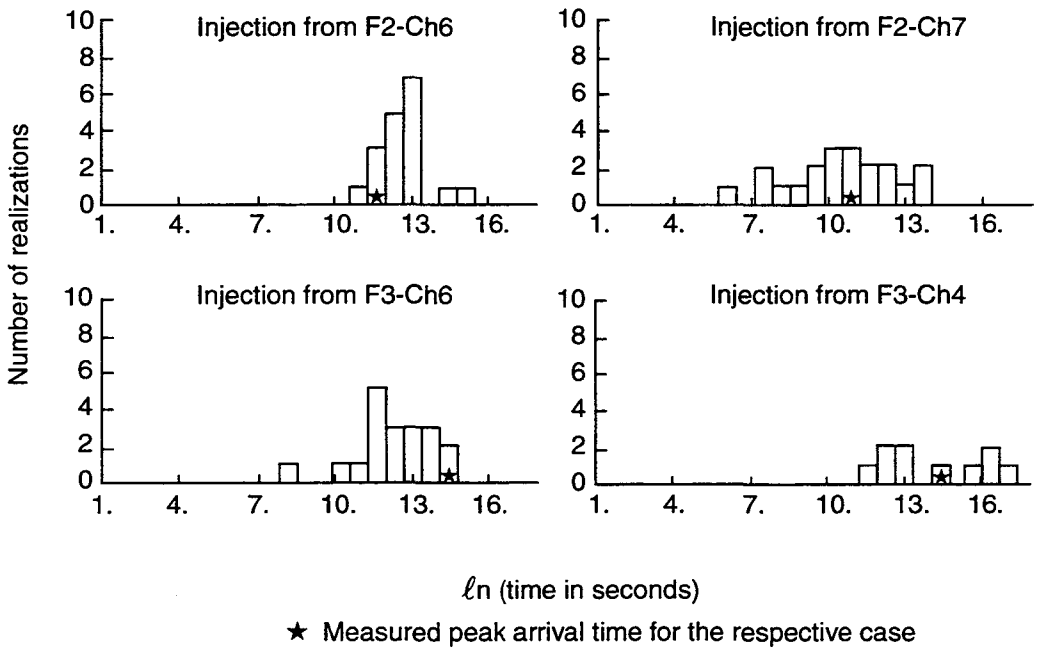

Figure 26. Histograms of the time of the peak arrival associated to the four sets of simulations of the tracer injections (after calibration). (Taken from Cacas et al., 1990.)

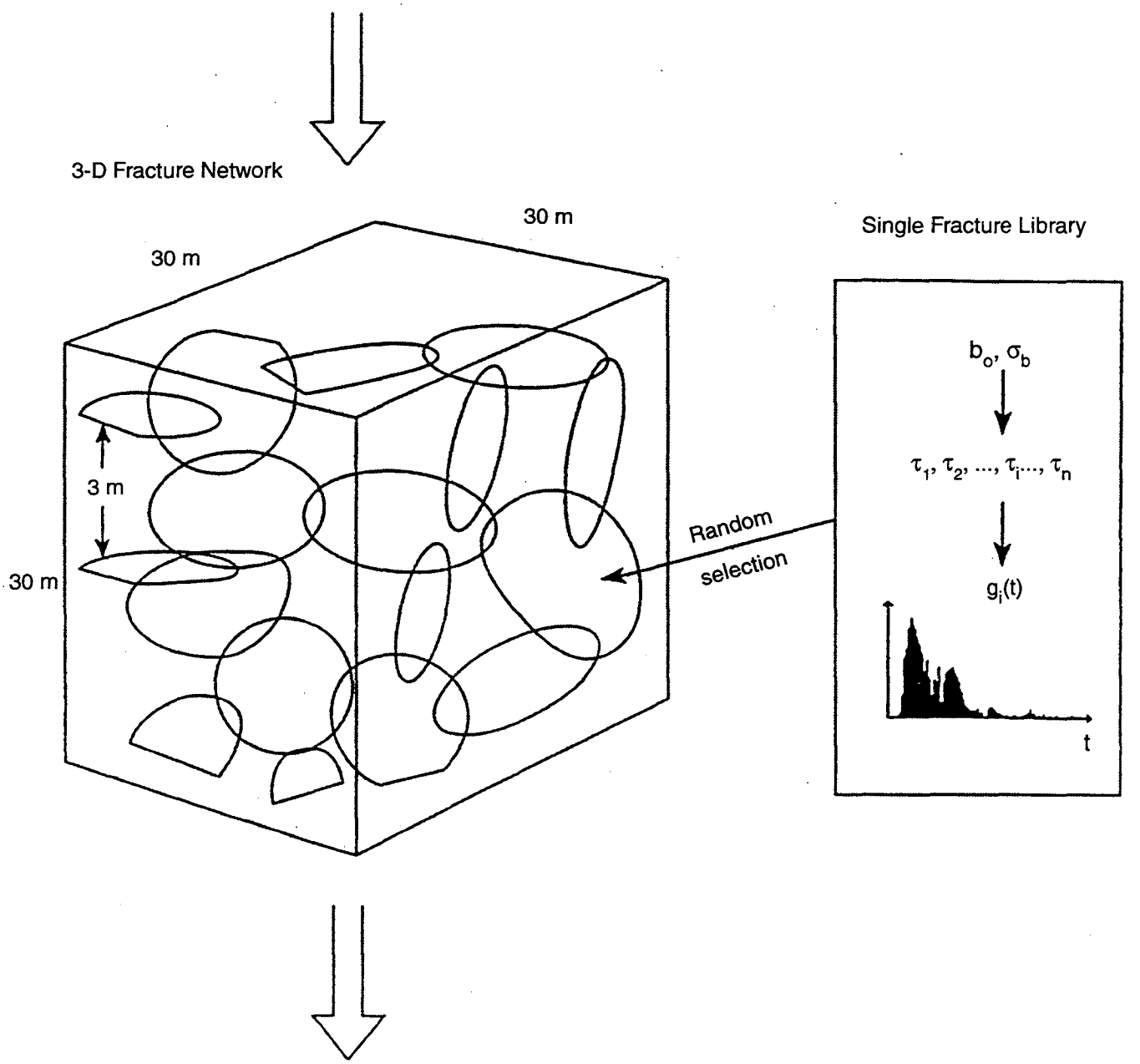

Figure 27. Conceptual model of a 3-D fracture network model, including effects of variable apertures within each of the fractures. (Taken from Nordqvist, et al., 1992.)

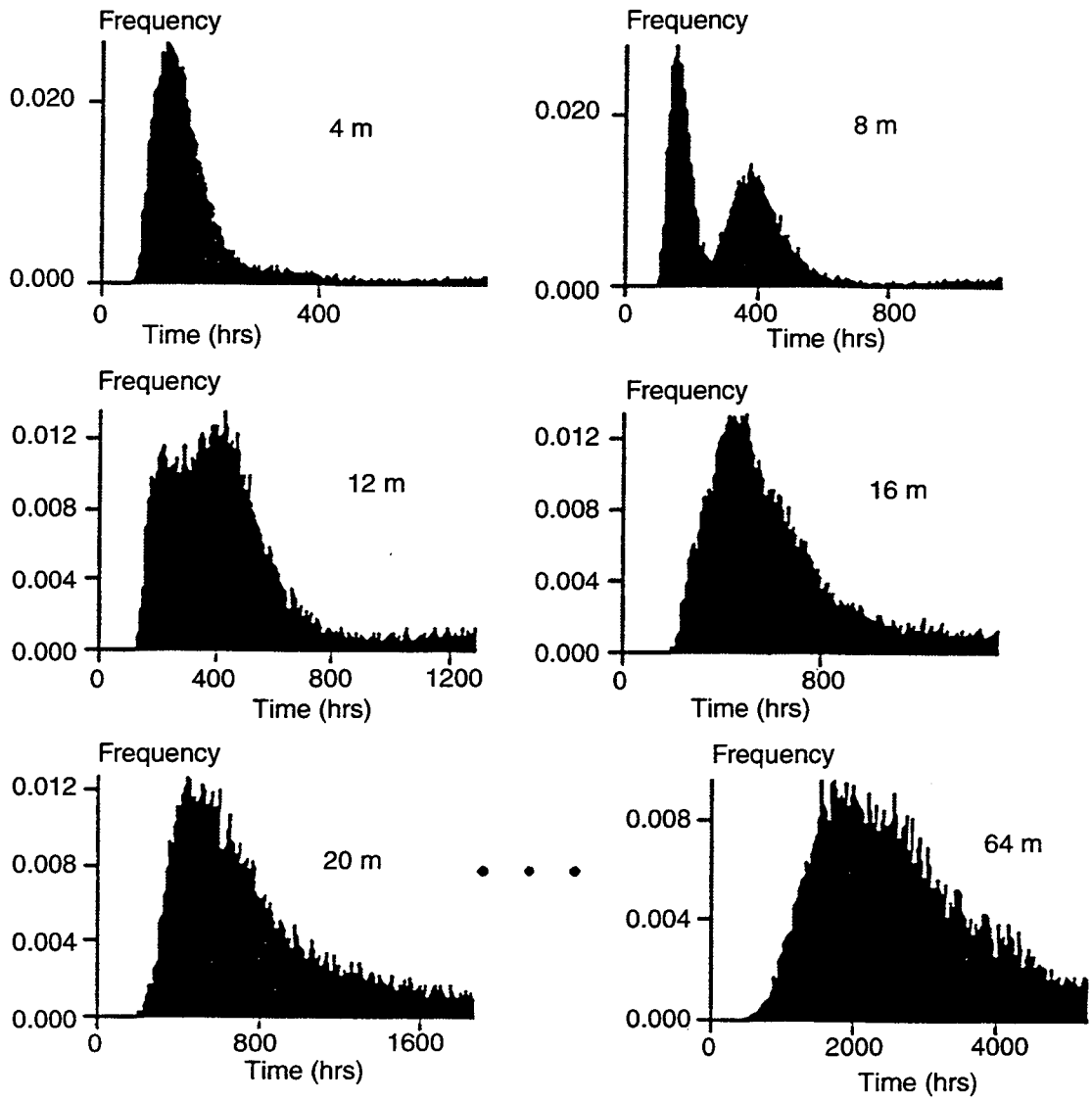

Figure 28. Calculated tracer breakthrough curves as a function of transport distance from a variable-aperture fracture network model. (Taken from Nordqvist et al., 1992.)

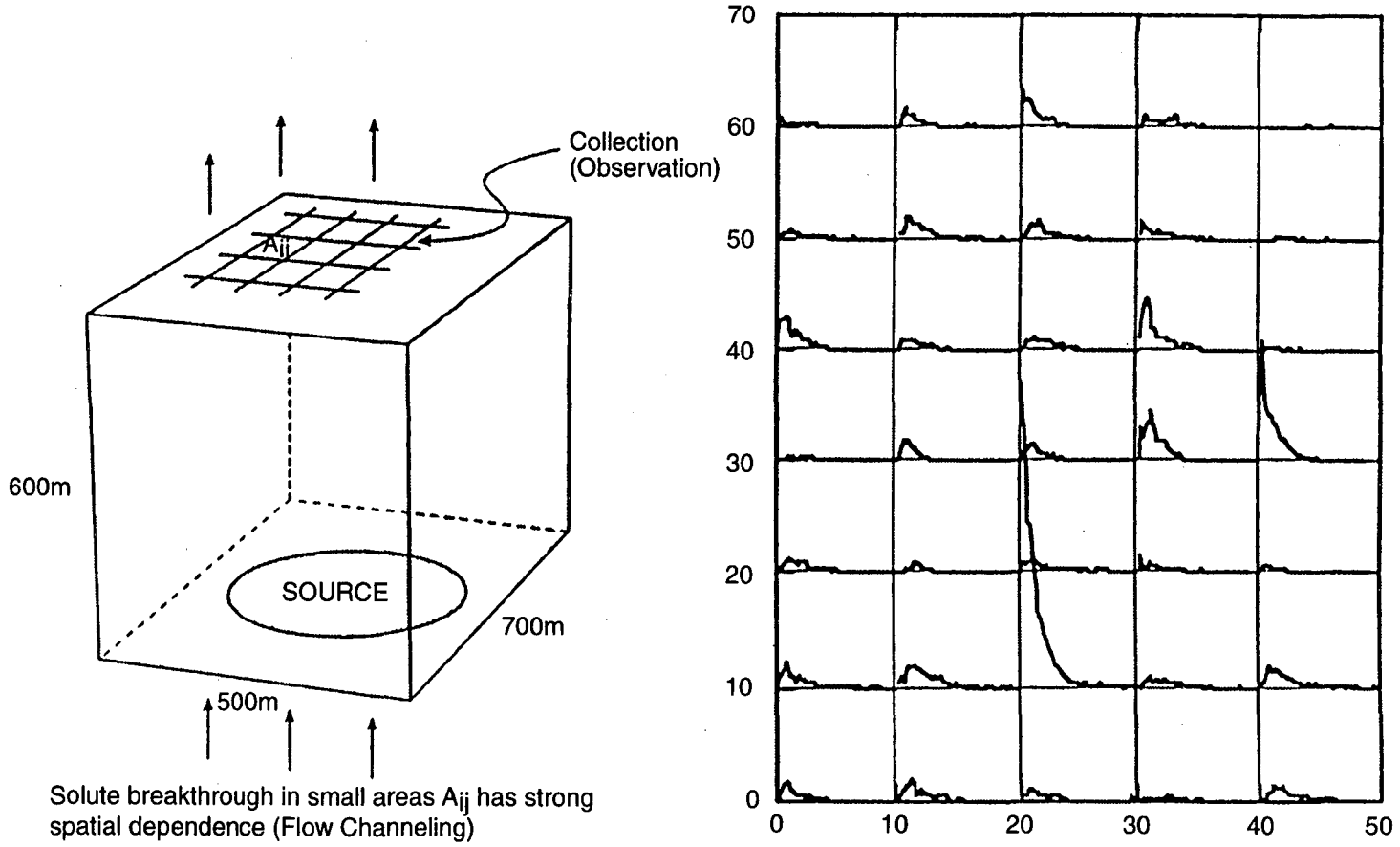

Figure 29. Schematic diagram (left) of flow from bottom to top in a block of heterogeneous fractured porous medium, and calculated breakthrough curves (right) in 35 100×100 m^2 outflow areas on the top exit plane. (Taken from Tsang and Tsang, 1996.)

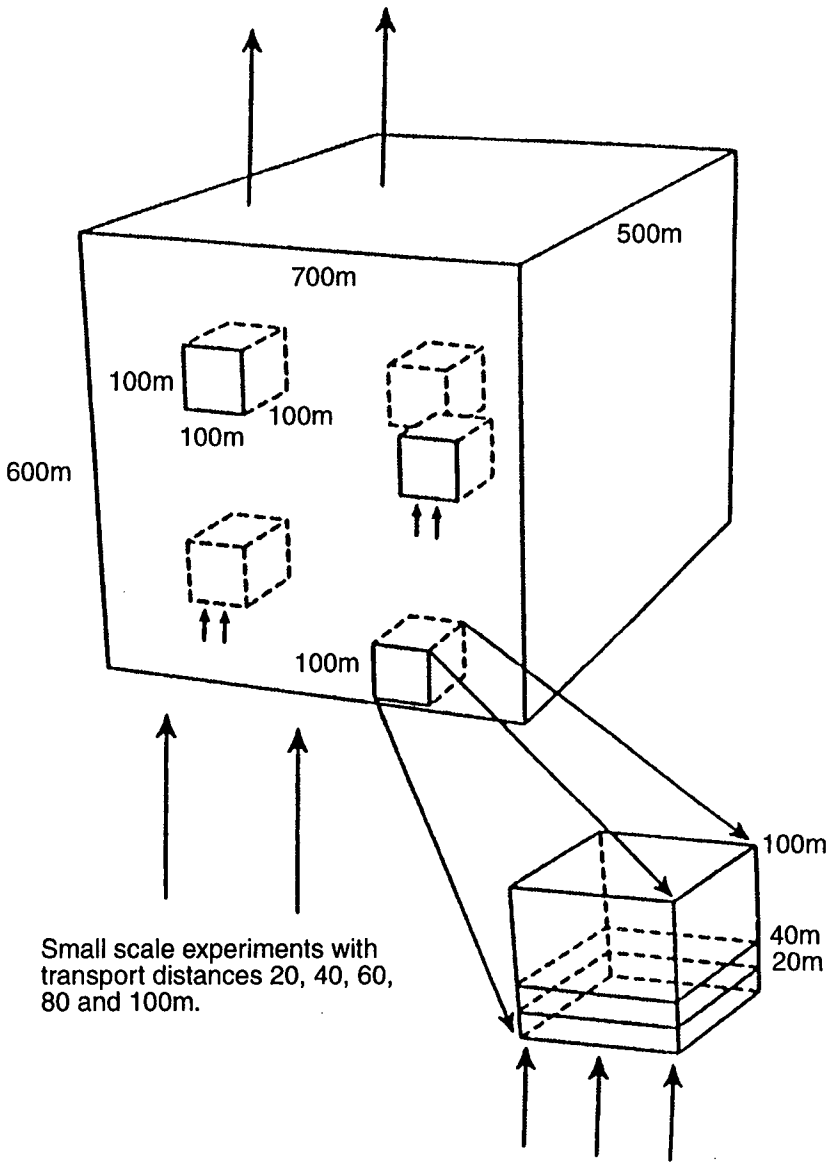

Figure 30. Schematic diagram suggesting small-scale natural gradient experiments within the $500 \times 700 \times 600$ m^3 block of heterogeneous porous medium. (Taken from Tsang and Tsang, 1993.)

Ernest Orlando Lawrence Berkeley National Laboratory
One Cyclotron Road | Berkeley, California 94720

Prepared for the U.S. Department of Energy under Contract No. DE-AC03-76SF00098